A Dynamic-Stiffness Hydrogel Platform Utilizing Phytochrome B and Phytochrome Interacting Factor 6 as a Light-Inducible Crosslinker

by

Nahyun Cho

A dissertation submitted in partial satisfaction of the

requirements for the degree of

Doctor of Philosophy

in

Chemical Engineering

in the

Graduate Division

of the

University of California, Berkeley

Committee in charge:

Professor Lydia Sohn, Co-chair
Professor David Schaffer, Co-chair
Professor Sanjay Kumar
Professor John E. Dueber

Fall 2018

A Dynamic-Stiffness Hydrogel Platform Utilizing Phytochrome B and Phytochrome Interacting Factor 6 as a Light-Inducible Crosslinker

Abstract

A Dynamic-Stiffness Hydrogel Platform Utilizing Phytochrome B and Phytochrome Interacting Factor 6 as a Light-Inducible Crosslinker

by

Nahyun Cho

Doctor of Philosophy in Chemical Engineering

University of California, Berkeley

Professor Lydia Sohn, Co-chair

Professor David Schaffer, Co-chair

Traditional cell culturing methods are generally static with respect to mechanical properties unlike *in vivo* conditions, suggesting that the results from *in vitro* experiments form an incomplete picture for downstream studies. My cell culturing platform utilizes phytochrome B (PhyB) and phytochrome interacting factor 6 (PIF6), plant proteins derived from *A. thaliana* which associate or dissociate based on two distinct wavelengths of light, as a controllable, reversible crosslinker within a hydrogel platform.

Both PhyB and PIF6 were created in bulk within *E. coli* and purified via Ni-NTA, ion exchange, and size exclusion columns. The *ex vivo* activity of my synthesized proteins was tested via total internal reflection fluorescence (TIRF) microscopy. A hyaluronic acid (HyA) polymer gel was chosen as the base of the cell culturing platform for both its biological compatibility and its ability to be modified for protein conjugation. A semi-interpenetrating polymer network (semi-IPN) matrix was made by creating a base HyA hydrogel through thiol-ene click chemistry and incorporating a free HyA polymer stand which was modified to have methacrylate groups for protein conjugation. The modification of the HyA polymers was confirmed via proton nuclear magnetic resonance (^{1}H NMR) spectroscopy. Confocal microscopy confirmed the covalent conjugation of fluorescently-labeled PhyB and PIF6 to the cell culturing platform. To confirm compatibility of the platform for cell culture, human mesenchymal stem cells were cultured for six days on the platform.

Atomic force microscopy (AFM) was used to measure the stiffness changes in the hydrogel platform when exposed to different wavelength light and preliminary data shows promising stiffness changes based on light cues. Future work on the platform will include establishing and characterizing the material properties of the hydrogel platform after variations are made on polymer lengths, protein density, and light intensity or duration. Upon optimization, this dynamic hydrogel platform could be utilized to mimic a variety of mechanical conditions found *in vivo* and provide insight to mechanobiological phenomena.

Table of Contents

List of Figures

List of Tables

Acknowledgements

The work of this dissertation would not have been possible without the support of many individuals. I would like to first and foremost acknowledge and thank my research advisor, Dr. Lydia Sohn, for her guidance and motivation throughout my doctoral research. Without her as my mentor, I could not have accomplished all that is presented in this dissertation. Additionally, I would like to thank Dr. David Schaffer for serving as my co-advisor throughout this journey. I would also like to express my profound gratitude to Dr. John Dueber for providing me his expertise, access to his laboratory facilities, and for serving on my dissertation committee. Finally, I would like to thank Dr. Sanjay Kumar for serving on my doctoral dissertation committee and providing me with his counsel.

I would like to recognize my friend and colleague, Tammy Hsu, who helped me both scientifically and emotionally. Without her, I could not have completed all the work in chapter three and subsequently the rest of the work presented in this dissertation.

I am forever grateful to the members of the Sohn Lab, who have always helped me with their scientific insight and camaraderie. I would especially like to recognize Roberto Falcon-Banchs, Junghyun Kim, and Olivia Scheideler, who have seen me through so many struggles and triumphs.

My undergraduate students also deserve their credit in both helping me in the lab and allowing me the privilege of mentoring them. Thanks to you all: Ilyssa Evans, Jimin Jasmine Lee, Justin Lee, Andrew Sum, and Hannah Tang.

My cheerleader, coach, and counselor, Long Le, has seen me through countless crises and late-night sessions. Your friendship throughout this process has been irreplaceable.

Finally, I would like to thank my mother, father, sister, and brother-in-law for their endless support throughout this process. I could not ask for a more supportive family.

Chapter 1. Dissertation Scope and Outline

This dissertation will demonstrate a dynamic, cell culturing platform that allows for controllable, reversible stiffness *in situ* while maintaining physiological conditions. Phytochrome B (PhyB) and phytochrome interacting factor 6 (PIF6) serve as a light-responsive, reversible crosslinker that would enable controlled change in hydrogel stiffness. Hyaluronic acid (HyA) hydrogel polymers are modified and functionalized with these proteins so that light cues can activate or deactivate the light-dependent protein-protein interaction to increase or decrease the density of crosslinks. Because this platform relies on a red/infrared light-based system, this hydrogel platform can create a highly tunable cell culturing system without compromising cell viability. This biomaterial would help obtain a fundamental understanding of the influence that temporal cell culture rigidity has on complex cellular phenomenon, such as cancer development, stem cell differentiation, and collective cell migration.

This dissertation is organized into the following chapters:

Chapter Two will focus on the motivation for the platform and previous work completed in the field of dynamic-stiffness cell culturing platforms.

Chapter Three will focus on the background and the creation of the PhyB and PIF6 proteins. Then, this chapter will confirm the exogenous protein activity of PhyB and PIF6.

Chapter Four will focus on the modification of hyaluronic acid gels and its ability to culture cells and conjugate proteins.

Chapter Five will focus on the material properties of the hydrogel platform as measured by atomic force microscopy.

Chapter Six will summarize the dissertation and provide suggestions for future work.

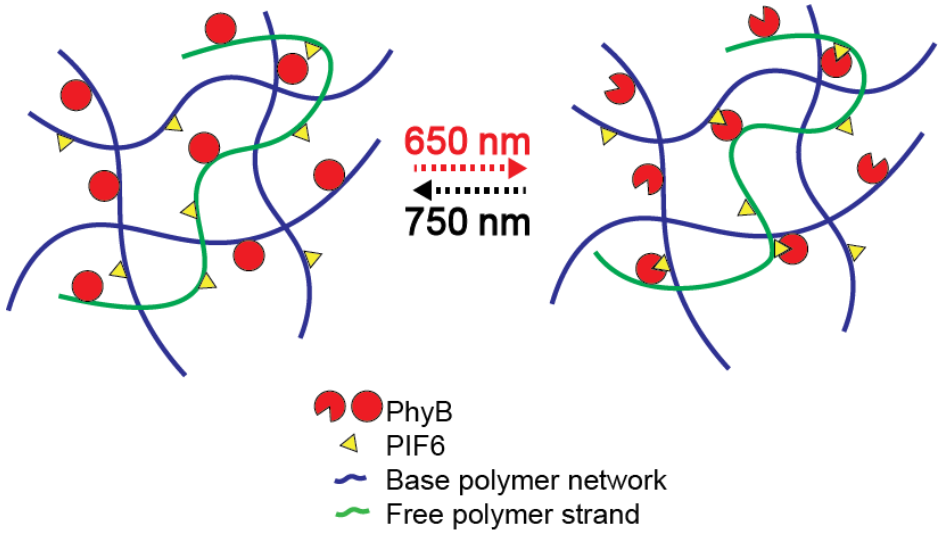

Figure 1. PhyB and PIF6-based hydrogel platform demonstration.

PhyB and PIF6 associate and dissociate to change the density of crosslinks within a hydrogel cell culturing platform.

Chapter 2. Introduction, Motivation, and Previous Work in the Field

2.1. How cells sense their mechanical environment

Within our bodies, our cells experience a diverse range of mechanical stimuli, such as shear, tensile, and contractile forces. The field of mechanobiology examines how the mechanical environment influences cellular processes and contributes to complex biological phenomena such as migration, development, and differentiation. The process by which a cell converts physical cues into a biochemical cellular response, or mechanotransduction, is dependent on a myriad of proteins including those on the surface of the cell that interact with the environment, intermediates that enhance signal sensitivity, and transcription factors that regulate gene expression.

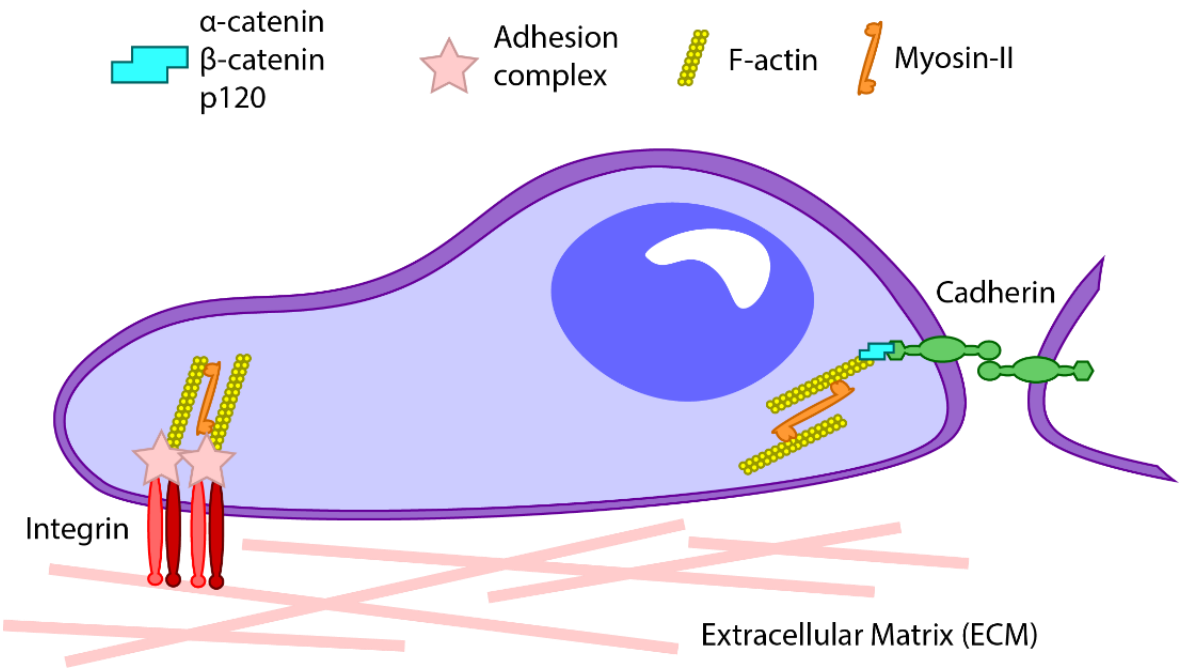

Figure 2. How cells sense their mechanical environment.

Integrins are transmembrane proteins that respond to adhesion motifs on the proteins found in the extracellular matrix (ECM). On substrates with increased stiffness, these integrins can form clusters and promote the polymerization of actin filaments. Cadherins are transmembrane proteins that have external domains which enable cell-to-cell mechanical influences and internal domains which connect to the F-actin filaments. The F-actin filaments can then propagate external physical stimuli or create forces on the cell's surroundings through actomyosin complexes.

Integrins are transmembrane proteins that are an integral part of focal adhesion complexes and interact with the proteins that make up the extracellular matrix (ECM), a network of macromolecules that provides structural support and biochemical cues for surrounding cells. On stiffer surfaces, the density of integrins increases which can lead to integrin clustering and start a cascade of downstream responses, such as promoting the polymerization of actin filaments. By increasing actin filament density, the tensile strength of the cell increases as well as the force potential of the cell to act on its surroundings. Actomyosin complexes, in which myosin proteins link and contract actin filaments, can be used to generate forces and to reinforce focal adhesion complexes by recruiting vinculin and talin proteins. [1,2] Another transmembrane protein, cadherin, is used to anchor to, receive signals from, and exert forces on adjacent cells. Cadherin clustering and conformational changes of its ectodomain regulate the actin cytoskeleton which connects to cadherin complexes through catenin proteins. These cadherin complexes enable cell-to-cell signaling and help direct multi-faceted and collective cellular processes such as cell migration, cell division, and wound healing. [3]

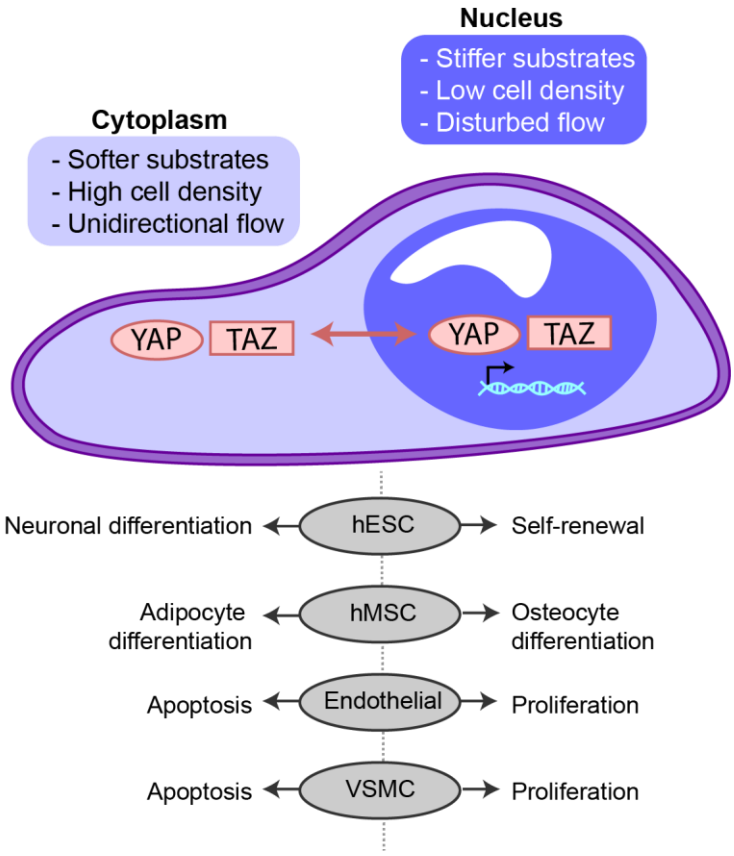

Figure 3. The effects of YAP/TAZ transcription factors localization in the cytoplasm and nucleus.

hESC, human embryonic stem cell; hMSC, human mesenchymal stem cell; VSMC, vascular smooth muscle cell. Adapted from [4,5].

Mechanosensing proteins allow the cell to feel external mechanical stimuli and influence the cytoskeletal structure to create responsive forces. Furthermore, these complexes can influence downstream processes by stimulating transcription factors to regulate genome expression. YAP (Yes-associated protein) and TAZ (a transcriptional coactivator with PDZ-binding motif) are two transcriptional regulators that are activated through increased tension in the actin cytoskeletal structure. Thus, when a cell is on a stiffer substrate, increased F-actin filament concentration and actomyosin contractile tension promote the colocalization and activity of YAP/TAZ in the nucleus. Many of the downstream effects of YAP/TAZ create positive feedback loops, such as

increasing the transcription of integrins and focal adhesion proteins. Specifically, YAP/TAZ activation and deactivation has been shown to be instrumental in triggering differentiation and proliferation of stem cells. (Figure 3) [4,5]

In addition to the activation of transcription factors, external mechanical cues can directly, physically influence the nucleus through the cytoskeleton as well. Linker of nucleoskeleton and cytoskeleton (LINC) complexes span the nuclear membrane and can translate physical stimulation felt from adhesion complexes and cell-to-cell junctions directly to the nucleus. These LINC complexes are connected to the cytoskeleton via nesprin proteins, which have KASH (Klarischt-ANC-1-SYNE homology) domains which are connected to actin, microtubules, and intermediate filaments. Because mechanical forces can directly interact with the nucleus, there is the possibility that physical cues can directly influence genetic expression through mechanical modification of chromatin structures. [6]

2.2. The role of stiffness on cellular processes

Understanding how cells utilize their mechanical environment to influence or direct its cellular processes would help develop insights into complex phenomena and diseases. Although individual cancer cells have generally been measured softer than non-cancerous cells, cancerous masses can create environments that are stiffer than the surrounding tissue by depositing excess ECM proteins, specifically collagen. [7] For breast cancer cell line MDA-MB-231, matrix rigidity directly influences the osteolytic metastatic potential of the cells by increasing the production of parathyroid hormone-related protein (PTHrP), which is a prevalent marker in bone metastases, on stiffer substrates. [8] Beyond sensing and responding to general substrate stiffness, cells can also determine gradients of stiffness to migrate accordingly in a process known as durotaxis. In the process of durotaxis, focal adhesion complexes and local arrangement of mechanosensing proteins can polarize the cytoskeleton to promote directed migration. Understanding the process of durotaxis and cell migration could help illuminate key factors in unknown processes such as cancer metastasis. [9]

In addition to increasing the metastatic potential of cancer cells, stiffness may also play a part in the early development of cancerous growth. In Chaudhuri et al. [10], normal mammary epithelial cells exhibited drastically different phenotypes when presented with different stiffness ECM. On softer surfaces (~30 Pa), the cells stopped proliferating and formed characteristic circular formations known as acini, while on harder surfaces (~300 Pa) the non-cancerous cells were proliferating, unable to form the acini structures, and invading the culturing matrix. While the stiffer substrates elicited cancerous phenotypes, the study did emphasize that the composition of the matrix could counteract the effects of stiffness. Increasing the concentration of laminin, which correspond to α6β4 integrin, over the concentration of RGD-motif containing proteins, which correspond to α_v- and β1-containing integrins, enabled normal phenotype of the mammary cells at the higher stiffness cell cultures. The study theorized that higher stiffness substrates did not allow for clustering of the α6β4 integrins. However, increasing laminin concentrations in the

matrix enabled higher densities and restored the clustering potential of α6β4 integrins, allowing the cells to active downstream regulators to form the acini structures.

Other than cancer progression, stem cell development and tissue progression is a complex and nuanced field that is also profoundly influenced by mechanical cues. Soluble and chemical factors have long been understood as important contributors to stem cell renewal and differentiation. However, understanding the exact influence of mechanical cues, and specifically stiffness, on how stem cells create differentiated populations could help more accurately recreate specific stem cell niches which would further the tissue engineering field.

In a landmark paper by Engler et al., [11] human mesenchymal stem cells (hMSCs) were found to differentiate into osteogenic (0.1-1 kPa), myogenic (8-17 kPa), and neurogenic (25-40 kPa) lineages depending on the stiffness of the cell culturing substrate. These results were further astounding as the cells continued expressing differentiation markers based on its original culturing stiffness even after presentation with contradictory soluble cues for other lineages. Furthermore, the hMSCs demonstrated a “mixed phenotype” when presented with these contradictory cues as opposed to creating two distinct populations of differentiation. Additionally, the study utilized blebbistatin, a nonmuscle myosin II blocking agent, to confirm that nonmuscle myosin II is required to have stiffness-driven differentiation. This paper demonstrated that substrate stiffness had a comparable, if not more important, influence on stem cell differentiation as soluble factors had.

Another example of the influence of matrix rigidity on stem cell development, adult neural stem-cells (aNSCs) have been found to favor different lineages based on the culturing substrate stiffness. Softer substrates (100-500 Pa) favored neuronal differentiation while harder substrates (1kPa-10kPa) promoted glial cells differentiation. In addition, when the aNSCs were cultured on substrates far beneath natively found stiffnesses (<10 Pa), aNSC proliferation, spreading, and differentiation were inhibited. [12] These findings further solidified the instrumental role that stiffness and mechanical cues have on stem cell differentiation and proliferation.

Since stem cell differentiation is multi-faceted, the influence and contribution of mechanical factors as compared to ligand presentation was investigated in Rape et al. [13] In this study, cells were exposed to a gradient of fibronectin concentration and stiffness (0.5-1.5 kPa) simultaneously to look for synergistic effects of these factors. Specifically, expression of microRNA miR18a, which is an oncogenic marker and highly upregulated on stiffer surfaces, was utilized to determine the influence of matrix stiffness and fibronectin density on oncogenic differentiation. The study created a platform to enable a highly parallel method of determining the synergistic influences of both chemical and physical cues. In doing so, they found that the miR18a expression regulation was complex and highly nonlinear. When culturing hMSCs on the platform, it was determined that osteogenic lineage determination was due to a combination of both fibronectin density and substrate stiffness while adipogenic differentiation was much more strongly influenced by substrate stiffness alone. This study demonstrates a necessity for engineering methods to create a diverse set of mechanical and chemical environments, to compare physical and chemical contributions, and to enhance our understanding of their synergistic effects.

Beyond imitating the inherent stiffness in tissues, many biological processes require cells to experience dynamic stiffnesses. Additionally, the timescale of these processes can range from slower, such as the increasing stiffness of the subventricular and ventricular zones in brain development [14], to more rapid changes in the mechanical environment, such as cyclical stresses found in the expansion and contraction of the endothelial lining in our blood vessels to regulate blood pressure. The diversity of biological mechanical stimuli that cells experience ranges not only in magnitude but temporally as well.

Evidence that temporal matrix rigidity affects stem cells differentiation was shown through proof of hMSCs "memory". Yang et al. [15] altered the stiffness on which hMSCs were cultured from 10 kPa to 2 kPa on days 1, 3, 5, 7, and 10. Over the course of 20 days, they observed the cells for the activation and localization of YAP/TAZ in the nucleus and expression of RUNX2, a pre-osteogenic marker. They found that there is a threshold time of 10 days in which exposing hMSCs to a stiff hydrogel will commit the lineage of hMSCs to osteoblasts, while softening the gel beforehand will allow for reversibility in cellular differentiation. The time-based influence of the substrate stiffness demonstrates the need for dynamic and finely temporally tunable stiffness platforms for culture. Engineering more complex, mechanically-stimulating environments will enable a multi-faceted approach to cell culture and can lead to higher throughputs of mechanobiology discoveries that were previously more nuanced.

2.3. Hydrogels as a cell culturing method to more closely mimic *in vivo* stiffnesses

Traditionally, our understanding of cellular biological phenomena has been based on our examination of cells cultured outside of the human body. Cells are plated on top of a glass or plastic petri dish and left in a static culture with minimal changes to its mechanical environment. However, within our bodies, there is a spectrum of stiffness that a cell could experience from very soft (i.e. neuronal tissue, <1 kPa) [16] to very stiff (i.e. collagen fibers, ~100 MPa) [17]. Glass and plastic surfaces have stiffness (>1GPa) that far exceed those found naturally and generally do not imitate inherent heterogenous stiffness variation found in tissues.

Because current cell culturing methods are generally static with respect to mechanical properties unlike *in vivo* conditions, it suggests the results from *in vitro* experiments form an incomplete picture for biological phenomena. Understanding how cells process and respond to substrate stiffness is vital for a more holistic understanding of complex biological processes. Without introducing exogenous variables, engineering a cell culturing platform that can finely tune the mechanical environments of cells is therefore key to understanding the influence of biophysical cues.

As the influence of substrate stiffness becomes more apparent, hydrogels have become an appealing choice for cell culture. Hydrogels are synthetic matrices and their stiffness can be controlled predictably to mimic the natural environment found in tissues. There are some native ways of recreating *in vivo* conditions by utilizing purified ECM proteins such as laminin, collagen, or recombinant basement membrane (Matrigel) or

removing cells from tissues in a process called decellularization. These naturally derived matrices, however, have highly variable compositions and stiffnesses and are more susceptible to degradation from secreted proteases during cell culture than hydrogels are. [18,19]

Hydrogels can have finely tunable stiffnesses by increasing or decreasing the crosslink density. For example, polyacrylamide gels can easily be modified to have a large range of stiffness from as low as 500 Pa to as high as 10 kPa. [20] Additionally, side groups found on hydrogel polymer chains can be altered to allow protein-conjugation essential for cell culture. For example, introducing peptides with RGD-motifs are necessary for integrin recognition, which can create focal adhesions that are utilized for cell anchorage. [21] Because hydrogels can have both tunable stiffness and customizable peptide or ligand concentrations, hydrogels are a preferred method of creating a diverse range of situations that more closely mimic the mechanical and chemical environments of *in vivo* conditions.

Depending on the hydrogel polymer, there are multiple ways that a hydrogel can change its stiffness. Some hydrogels, like agarose, utilize physical crosslinks or entanglement of the polymer chains to create a solid-like structure. Other hydrogels have specific crosslinking reagents, such as bisacrylamide in polyacrylamide gels, necessary to create a covalent network. Furthermore, other hydrogels have reactive side groups that are susceptible to modifications to enable multiple types of chemical crosslinks or radical polymerization. [22] The influence of mesh size on culture should be considered when determining the polymer and crosslinking method, as many hydrogel platforms change stiffness as a function of mesh size. [18] The diversity of hydrogels that allow different stiffnesses and peptide presentations while maintaining a physiologically stable environment makes hydrogels a prime candidate to study mechanobiology.

2.4. Dynamic-stiffness hydrogel platforms to study mechanical influences on cellular processes

There are a couple of noteworthy advancements in the field of dynamic-stiffness hydrogel platforms. Mosiewicz et al. [23] created stiffening polyethylene glycol (PEG) gels through thiol-ene reactive-crosslinkers that have degradable protecting groups upon ultraviolet (UV) light exposure. With these gels, they observed hMSCs migrate in gradient stiffnesses. Furthermore, they discovered that hMSCs exhibited durotaxis when exposed to high stiffness gradients (i.e. 5.5 – 8.0 kPa) but not when exposed to lower gradients (i.e. 3.0 – 5.5 kPa). Similarly, Guvediren & Burdick [24] also utilized gels that can stiffen, via radical chemistry, from 3 kPa to 30 kPa to observe the influence of temporal rigidity on differentiation. They used their platform to test the effects of stiffening after 1, 3, and 7 days of culture on adipogenic differentiation and found that the longer hMSCs are cultured on a soft surface, the more likely it is for them to express adipogenic markers (i.e. FABP4, PPRG). Another platform developed in Kloxin et al. [25,26] was a PEG-based hydrogel that can soften up to 78% of the hydrogel stiffness (i.e. 32 kPa to 7 kPa) via a crosslinker that degrades when exposed to 365-420 nm UV light. These platforms advantageously eliminate the need for passage, an inherently disruptive process, to change the physical environment of the cells. While these platforms allowed for a more

dynamic cell culturing method, the changes in stiffness were not reversible which limits the biological conditions they can mimic. Additionally, the utilization of UV light, albeit short, is less ideal as UV in high doses can cause DNA damage and be toxic to cells.

Rammensee, et al. [27] went one step further and developed a platform that can create reversible-stiffness changes by utilizing complementary DNA strands. The polyacrylamide hydrogel intrinsically had two "sidearm" sequences. A bridging complementary strand linker (L) with a toe-loop was introduced to create a DNA-based crosslink. By introducing a second "release" (R) complementary strand, the L strand thermodynamically preferred to bind to the R strand over the two "sidearms", thus relieving the hydrogel platform and creating a less stiff structure. Their reversible-stiffness hydrogel, however, changed stiffness on the order of hours, which limited the platform's ability to mimic all *in vivo* conditions, which have a variety of temporal stiffness changes.

Platform	Unidirectional or Reversible	Patterning capabilities	Time scale of change
Mosiewicz et al. [23]	Unidirectional hardening. Crosslink density increases when UV light degrades protecting groups to expose reactive crosslinks.	Patterning capable based on UV light	Rapid (~1 min)
Guvediren & Burdick [24]	Unidirectional hardening. Crosslink density increases via UV-activated photoinitators that start radical polymerization.	Patterning capable based on UV light	Rapid (~10 min)
Kloxin et al. [25,26]	Unidirectional softening. Crosslink density decreased when exposed to UV light to degrade UV-degradable crosslinks.	Patterning capable based on UV light	Rapid (0-8 min)
Rammensee et al. [27]	Reversible stiffness. Crosslink density changed based on presence of DNA strands.	No patterning capabilities	Long (2-9 hours)

Table 1. Summary of current methods for dynamic stiffness hydrogels.

2.5. Proteins as a dynamic crosslinker for hydrogels

A dynamic-stiffness cell culturing platform is critical for examining the contribution of matrix rigidity on cellular processes and phenotype. Because cell passage is an inherently disruptive process, multiple dynamic hydrogel platforms have been developed with the capabilities of changing stiffness *in situ*. In addition to the methods described in the previous section, some platforms utilized protein interactions to serve as a dynamic crosslink. In Miyata et al. [28,29] antibodies (Rabbit IgG) and secondary antibodies (Goat anti-Rabbit IgG) were utilized to serve as a dynamic crosslink within a polyacrylamide and polyacrylic acid hydrogel. Goat anti-Rabbit IgG was covalently bonded to the polymer strands and Rabbit IgG, its antigen, served as a crosslink between the polymer strands. Adding additional free-floating Goat anti-Rabbit IgG would release the Rabbit IgG from

the polymer strands through competitive binding and create a more porous hydrogel network. Lu et al. [30] similarly created *N*-isopropylacrylamide hydrogels with anti-fluorescein antigen-binding (Fab') fragments covalently bonded to the polymer strands. The addition of fluorescein or fluorescein-tagged spacer units allowed for structural modification to the hydrogel.

In a different approach, Rombouts, et al. [31] utilized silk-stranded collagen that will either bind or unbind based on the temperature at which the material is heated. As the protein was cooled, the protein experienced a conformational change that allowed the collagen strands to form a triple helix structure. By creating these triple helix structures, the proteins formed temporary bonds that increased the density of crosslinks and generated a stiffer hydrogel. In a similar fashion, Wang et al. [32] utilized coiled coils, a structural motif where multiple alpha helices create a supercoil, to create a dynamic hydrogel crosslink. In this platform, a portion of the protein kinesin (amino acids 336-590) was incorporated into the hydrogel polymers which created hydrogels that softened above 39°C, due to denaturation of the proteins.

These protein-based methods of dynamic crosslinking relied on creating environments that shifted the protein conformational state. Besides temperature, pH or salinity could also shift proteins into different conformational states. King et al. [33] developed a polyethylene glycol (PEG)-based hydrogel microparticles that had calmodulin mutant (T34C, T110C) proteins attached to the polymer strands. The protein would aggregate or disaggregate based on the pH of the environment and caused changes in the hydrogel properties based on the magnitude of shift from the protein's isoelectric point at pH 4.2, with the gels becoming more porous at higher pH and denser at lower pH solutions.

These gels, however, are all unsuitable for cell-culture because of the drastic changes in temperature or pH which is unlike physiological conditions. Cells *in vivo* generally are maintained within a homeostatic environment, so these platforms would not be suitable for studies with cell lines that are sensitive to dramatic changes. Although the platforms from Miyata et al. [28,29] and Lu et al. [30] remained at physiological conditions, both suffered from mass transport limitations as changing the material properties required the diffusion of antigens. These platforms were unfavorable methods to study the effects of rapid changes in substrate stiffness on cellular processes. To utilize proteins as a dynamic crosslink, a protein must be inducible into different conformational that does not require changing the cell culturing environment beyond physiological conditions.

2.6. Discussion

The influence of the mechanical environment on cells is interpreted through many dynamic biomolecular components, such as transmembrane proteins, actin filaments, and transcription factors. Specifically, transmembrane proteins create a physical bridge for external cues to affect the cytoskeleton of the cells. For example, integrins bind to adhesion motifs found in the ECM and cadherins respond to adjacent cells. These transmembrane proteins can then form clusters or change conformation to trigger downstream processes such as actin polymerization or YAP/TAZ activation. Through

LINC complexes, the cytoskeleton is directly connected to the nucleus, suggesting that physical cues can even directly regulate gene expression by mechanically modulating the nucleus.

The stiffness cells experience can influence a multitude of complex cellular processes including the development of cancerous masses and metastasis. On stiffer substrates, normal mammary epithelial cells elicited cancerous phenotypes, such as excess proliferation and matrix invasion, [10] and breast cancer cells demonstrated an increased production of hormones that are associated with bone metastasis [8]. In addition to affecting cancer phenotypes, stiffness has been shown to be an instrumental influence in stem cell differentiation and proliferation. Engler et al. [11] was able to promote various hMSC differentiation markers by varying stiffness and could even contradict the influence of soluble cues. Likewise, aNSCs promoted various lineages based on substrate stiffness, with softer substrates promoting neurons and stiffer substrates promoting glial cells. [12]

Beyond looking at stiffness in isolation, Rape et al. [13] engineered a cell culturing platform and found synergistic, non-linear effects of ligand presentation, specifically fibronectin, and stiffness on hMSC differentiation. Furthermore, Yang et al. [15] found that hMSCs have “memory” and that hMSCs cultured on stiffer surfaces for a threshold of ten days led to permanent YAP/TAZ localization in the nucleus. Both studies suggested that the influence of matrix rigidity on differentiation is nuanced and will require newly engineered cell culturing platforms to study them.

Hydrogels are a commonly used material to study the effects of stiffness on cellular processes. Not only can hydrogels be modified to present various necessary peptides and adhesion motifs, they can also have tuned stiffness based on crosslinker chemistries and concentrations. The customization and biocompatibility of hydrogels make them ideal materials for creating engineered cell culturing platforms.

Many have created dynamic-stiffness hydrogel platforms to study the effects of stiffness on cellular processes. For example, some have utilized UV light to create hydrogels that stiffen [23,24] or soften [25,26] upon exposure to light cues. While these platforms were able to create quick, patternable stiffness changes, these changes were only unidirectional. Others have implemented DNA [27] or antibodies [28-30] to serve as a dynamic, reversible crosslinker, but these methods were limited by diffusion to create quick stiffness changes. Finally, protein-protein interactions have also been employed for use as a dynamic crosslinker, by activating or deactivating their association through changes in temperature [31,32] or pH [33]. While controllable, these platforms required dramatic changes that go beyond physiological conditions which made them unfavorable for studying influences of stiffness on sensitive cell lines.

To study the influence of matrix rigidity on cellular processes, a dynamic hydrogel crosslinker must be engineered that does not require dramatic environmental changes. This dissertation demonstrates the ability of optogenetic proteins PhyB and PIF6 to serve as a reversible, dynamic crosslinker. Because their reversible association can be modulated through light, incorporation of PhyB and PIF6 as a light-inducible crosslinker in a hydrogel can serve to have many advantages when making a dynamic-stiffness platform. It has the potential for patterned stiffnesses, the ability to respond quickly to light stimuli, and the biocompatibility necessary for cell culture with sensitive cell lines.

Chapter 3. Phytochrome B (PhyB) and Phytochrome Interacting Factor 6 (PIF6) as a Light-Inducible Crosslinker

3.1. Introduction: Optogenetic proteins

Light-sensitive proteins are favorable candidates to serve as a dynamic crosslink because its conformational change is controllable and cued with a bio-inert signal. Light immediately penetrates transparent mediums which allows for a quicker response time and overcomes limitations found in mass transport. [52] Previously, optogenetic proteins have been utilized for control of cellular function by conjugating these proteins to other proteins of interest. [53,54] In the context of a dynamic-stiffness hydrogel, these light-dependent proteins hybridize the advantages of the reversibility of the DNA-based hydrogel and the response time of the UV-degradable crosslink system.

Among the light-sensitive proteins, there are multiple potential candidates that have reversible associations. Cryptochrome 2 (Cry2) protein, which is responsible for maintaining circadian rhythm within plants and animals, creates aggregates when exposed to blue light and dissociates in the absence of blue light. [54-57] While this protein has a quick response time to blue light for its association, Cry2 is an aggregating protein meaning that the protein association is not as controllable as a dimerization or a binary interaction with another protein. Additionally, the dissociation is gradual and not distinctly controllable. The lack of the “off-switch” for Cry2 limits the ability of these proteins to help create a platform that has temporally-precise stiffness changes.

Other light-inducible proteins such as Dronpa were considered. Unlike Cry2, Dronpa has two distinct wavelengths to either induce or inhibit dimerization of the protein with itself. [54,58] This is more favorable than Cry2 and other gradually dissociating proteins because of the controllable nature of the dissociation. However, the wavelengths of these cues are close to the blue-light region. While light can be bio-inert, the closer the wavelength of light is to the blue spectrum, the more toxic it can be to cells as the high-energy of blue light lends to potential DNA damage. This makes Dronpa a less favorable candidate as the blue light may interfere with sensitive cell lines and limit the downstream applications of the hydrogel platform.

Phytochrome B (PhyB) and phytochrome interacting factor 6 (PIF6) are two plant proteins that associate and dissociate based on 650 nm and 750 nm wavelength light respectively. [52-62] Within PhyB, a cofactor phycocyanobilin (PCB) undergoes an isomerization and determines the red or far-red absorbing conformation of PhyB, abbreviated Pr and Pfr respectively. In *A. thaliana*, the Pfr freely binds to counter-parts such as PIF6 and forms a complex that can be transported into the nucleus of the cell to prevent sprouting. Unlike some of the other light-sensitive proteins, these proteins utilize the red and far-red light as cues, which are considerably less toxic than blue or UV light.

Levskaya et al. [63] utilized these proteins to recruit Rho-family GTPases, which control the actin cytoskeleton, to induce reversible morphological changes within cells. Furthermore, they modified the PhyB protein and created a remarkable robustness in the reversibility of their interactions with each other, associating and dissociating repeatedly (up to 100 times). The proteins also demonstrated fast kinetics for both association (1.3 ± 0.1 s) and dissociation (4 ± 1 s). For these reasons, PhyB and PIF6 were chosen to be the light-inducible crosslinker in our dynamic hydrogel system.

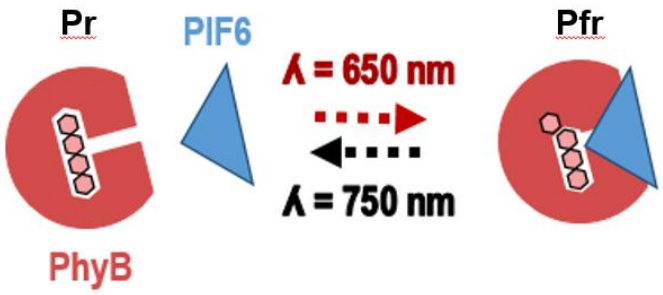

Figure 4. Phytochrome B (PhyB) interaction with phytochrome interacting factor 6 (PIF6).

PhyB has two conformational states, one that absorbs red light (Pr) and one that absorbs far-red light (Pfr). The PhyB binds with its partner, PIF6, when it is in the Pfr conformation.

3.2. Materials

Terrific Broth (TB), isopropyl β-D-1-thiogalactopyranoside (IPTG), arabinose, chloramphenicol (Cam), ampicillin (Amp), δ-aminolevulinic acid (ALA), HEPES, imidazole, Coomassie, sodium chloride, potassium chloride, magnesium chloride, and sodium hydroxide were purchased from ThermoFisher Scientific (Waltham, MA). Lysogeny broth (LB) and dithiothreitol (DTT) were purchased from Spectrum Chemicals & Laboratory Products (New Brunswick, NJ). Calcium chloride, glutaraldehyde, and (3-Aminopropyl) triethoxysilane (APTES) were purchased from Sigma-Aldrich (St. Louis, MO). Phosphate-buffered saline (PBS) was purchased from Life Technologies (Carlsbad, CA). Ethanol was purchased from Decon Laboratories (King of Prussia, PA). Ni-NTA superflow beads were purchased from Qiagen (Venlo, Netherlands).

3.3. Method: Protein production

3.3.1. Overview

All proteins were produced within the John Dueber Lab, University of California, Berkeley. Both proteins, PhyB and PIF6, were synthesized and purified via transformation into the BL21-DE3-Rosetta strain of *E. coli*. The template for the proteins was acquired via an Addgene library that had the specific Levskaya et al. [63] protein sequences. These proteins were utilized instead of the full PhyB protein as the paper had determined that PhyB (1-908) had a more robust reversible association with PIF6.

3.3.2. Expression and purification via *E. coli*

Different variants of plasmids that express the two central proteins required for this project were made via golden gate assembly, a unidirectional plasmid assembly method in molecular cloning that utilizes type IIs restriction enzymes. [64] PIF6 and PhyB were altered through recombinant DNA to express a fused fluorescent protein (e.g. eYFP, mTurquoise). The Dueber lab had previously cloned these tags in a MoClo Golden Gate format that allowed rapid and facile construction of these clones in parallel. [65,66] Similarly, different fluorescent proteins were easily interchanged at the cloning stage, as needed.

These plasmids utilized a T7 promoter and terminator sequence to enhance the expression of the proteins of interest. Additionally, a Lac Operon and Lac Inhibitor were also included so that the protein expression were controlled with the presence of Isopropyl β-D-1-thiogalactopyranoside (IPTG). There was a histidine tag on the C-terminus of both

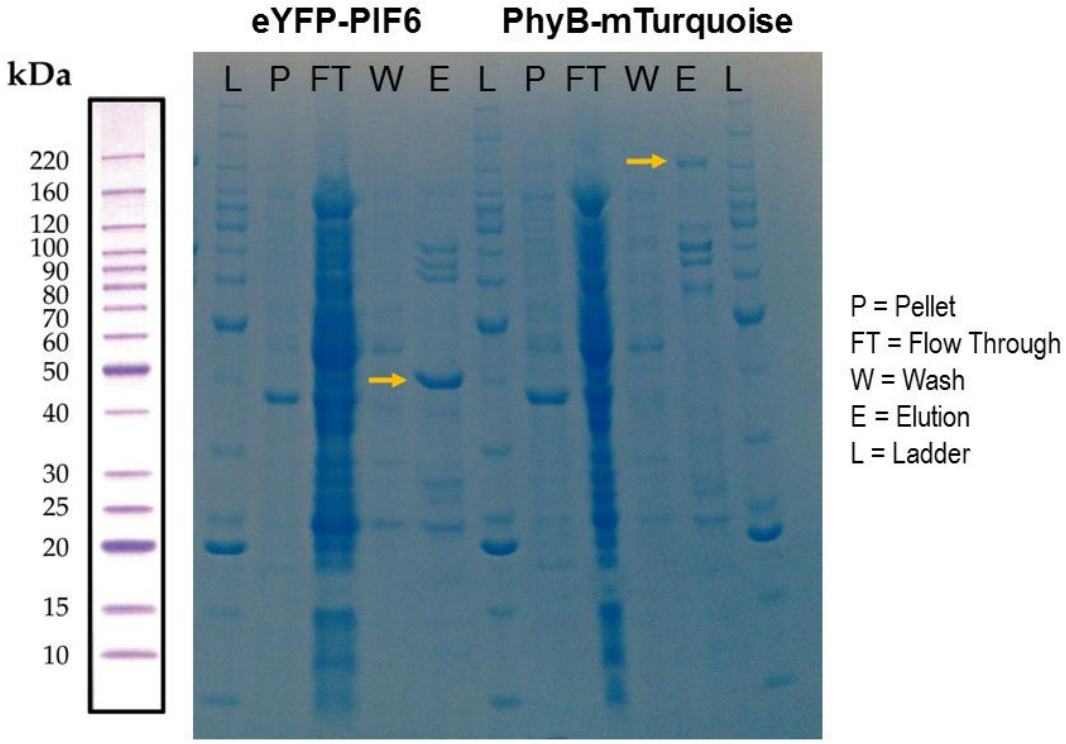

Figure 5. SDS-PAGE of eYFP-PIF6 and PhyB-mTurquoise fractions during Ni-NTA column purification.

The anticipated size of eYFP-PIF6 and PhyB-mTurquoise are 38. 5 kDa and 128 kDa respectively. The yellow arrow points to a strong band of protein approximately where the proteins are expected in the elution column. Benchmark™ Protein Ladder (Unstained) (ThermoFisher Scientific) is used as a protein ladder.

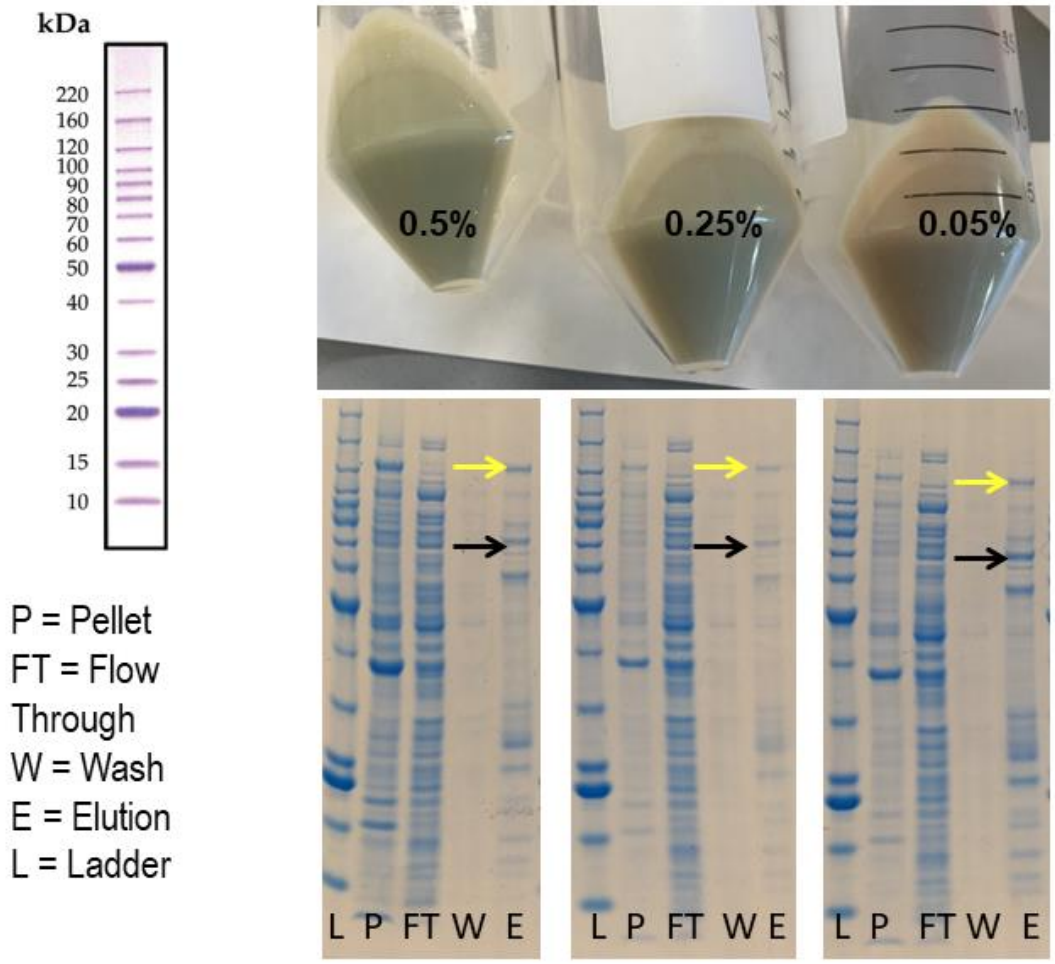

Figure 6. SDS-PAGE of and PhyB-mTurquoise fractions during Ni-NTA column purification upon varying arabinose concentrations.

The anticipated size PhyB-mTurquoise is 128 kDa. The yellow arrow points to a strong band of protein approximately where the proteins are expected in the elution column. Expression of PhyB was measured relative to the chaperonin protein found at 70 kDa (indicated with a black arrow). Visually 0.5 w/v% arabinose inductions show a greener hue, characteristic of the cofactor PCB. Benchmark™ Protein Ladder (Unstained) (ThermoFisher Scientific) is used as a protein ladder.

proteins to assist with purification through Ni-NTA columns. Both plasmids had been created for compatibility with BL21-DE-Rosetta *E. Coli* cultures. For the PhyB-mTurquoise, a plasmid that allowed the endogenous production of phycocyanobilin (PCB), a cofactor of PhyB, was cotransformed, as was standard in literature for PhyB production in *E. coli*. [67-69] This plasmid, which utilized a lac/ara-1 promoter which is activated by arabinose, produced two enzymes, hemeoxygenase-1 (HO1) and oxidoreductase (PcyA), to create endogenous PCB from heme molecules. This plasmid was a gift from Professor Lagarias at UC Davis.

The plasmids were transformed into BL21-DE3-Rosetta, a strain of *E. coli* that has chloramphenicol (Cam) resistance and has been designed to enhance the expression of eukaryotic proteins which contain codons that are rarely found in *E. coli*. The colonies were grown at 37°C on a shaker until the optical density (OD) at 600 nm was between 0.8-1. After cooling the culture, IPTG (1 mM) was used to induce the colonies to express the proteins.

For PhyB, arabinose was added to a final concentration of 0.5 w/v% to induce the production of PCB within the *E.* coli. Upon induction with arabinose, 100µM of δ-aminoleuvulinic acid (ALA), a precursor of PCB, was also added to PhyB cultures. These conditions were chosen based on results from optimization experiments. (Figure 6, 7) The cultures were incubated on the shaker at 18°C for 24 hours to allow for proteins to be expressed. The cultures were then spun down and frozen as a pellet until purification. The frozen pellets were resuspended in Buffer A (50 mM HEPES, 25 mM imidazole, 150 mM NaCl, and 1 mM DTT) and sonicated for a total of two minutes. Cultures were spun

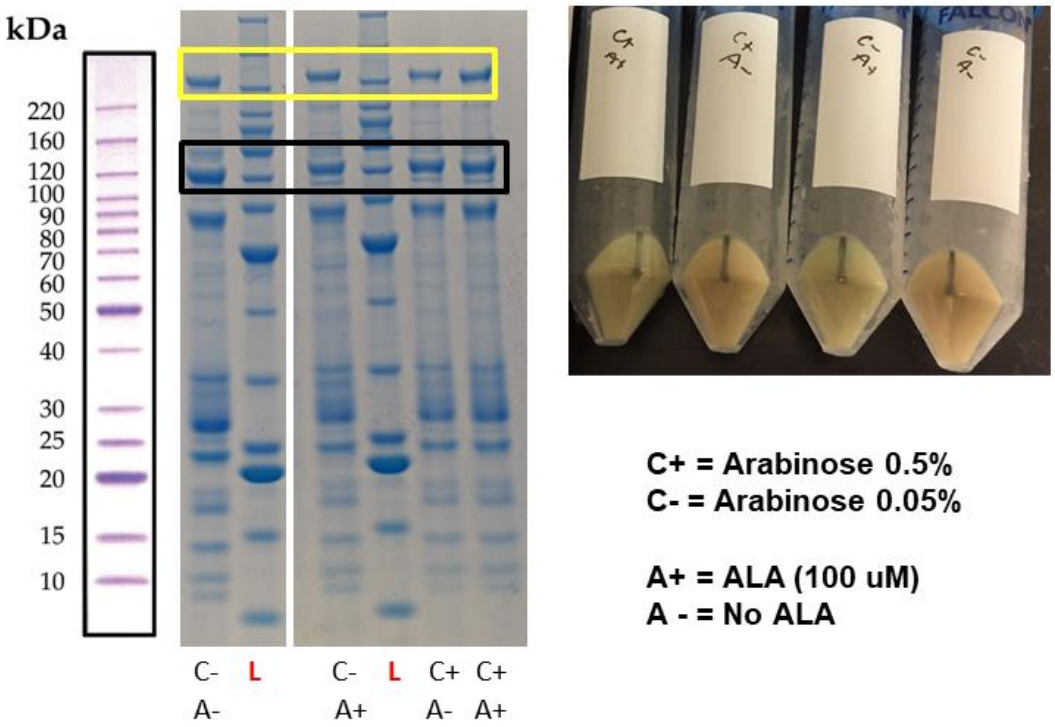

Figure 7. SDS-PAGE of and PhyB-mTurquoise fractions during Ni-NTA column purification upon varying arabinose and ALA concentrations.

The anticipated size PhyB-mTurquoise is 128 kDa. The yellow box shows a strong band of protein approximately in the area where the proteins are expected in the elution column. Expression of PhyB is measured relative to the chaperonin protein found at 70 kDa (indicated with a black box). Visually, inductions with ALA and 0.5 w/v% arabinose showed a much stronger green hue, typical of PCB production. Protein Ladder (Unstained) (ThermoFisher Scientific) is used as a protein ladder.

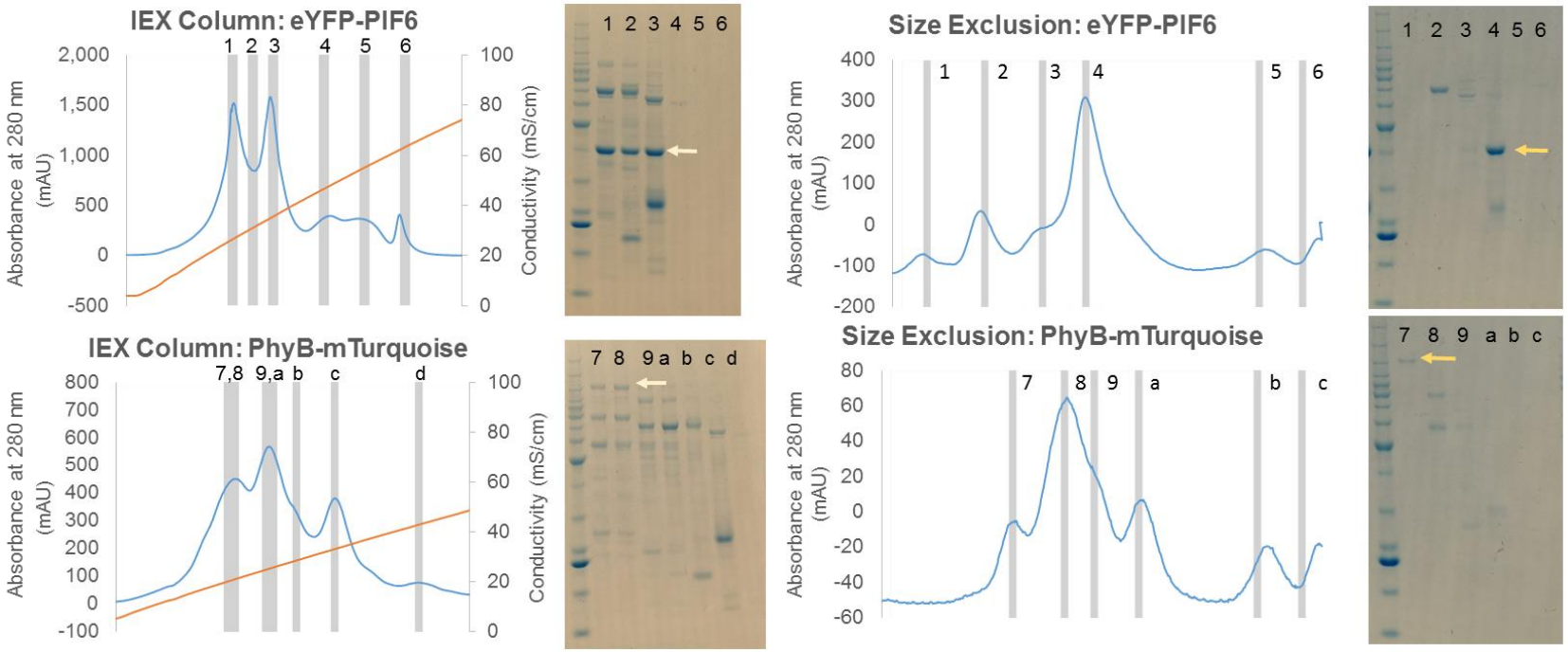

Figure 8. Purification of PhyB and PIF6 through ion exchange and size exclusion chromatography.

SDS-PAGE was utilized to monitor the presence of eYFP-PIF6 and PhyB-mTurquoise in fractions taken during (left) ion exchange and (right) size exclusion column purifications. Conductivity (orange) was utilized to monitor the NaCl concentration during purification with the ion exchange column. Absorbance (blue) at 280 nm was utilized to monitor protein concentration in both the ion exchange and size exclusion column purifications. The grey bands indicate where fractions were taken, and the corresponding SDS-PAGE columns have been labeled with numbers/letters. The arrows point to strong bands where the proteins are expected.

down at 10,000 RCF for 20 minutes at 4°C twice and the supernatant that was collected at the end served as the lysate, or flow through, solution.

Nickel-NTA columns were prepared and primed with Buffer A prior to exposure to the lysate solution. After the lysate solution was poured over the Ni-NTA beads, the column was subsequently washed with excess Buffer A to remove non-specifically bound proteins. The proteins were eluted off the columns by running Buffer B (50 mM HEPES, 500 mM imidazole, 150 mM NaCl, 5 mM DTT) over the column in three batches. The aggregating nature of fluorescently-tagged PIF6 and PhyB required a higher amount of reducing agent DTT (up to 5 mM) to separate the aggregates. After collecting fractions throughout this process, an SDS-PAGE (sodium dodecyl sulfate-polyacrylamide gel electrophoresis) gel stained with Coomaise was used to analyze the purification process.

SDS-PAGE gel analysis for the eYFP-PIF6 and PhyB-mTurquoise showed a distinct and strong band at the expected size of 38.5 kDa and 128 kDa, respectively. (Figure 5) The elution fraction from the Ni-NTA column purification was then purified further using FPLC and a combination of an ion exchange column (HiTrapQ HP, GE Healthcare Life Sciences) and size exclusion column (HiLoad 16/600 Supderdex 200pg, GE Healthcare Life Sciences). To create the purest PIF6 and PhyB proteins, ion exchange (IEX) fractions 1-3 and 7-8, respectively, were taken and purified with the size exclusion column. Finally, Fractions 4 and 7 from the size exclusion column served as the final PIF6 and PhyB fractions, respectively. (Figure 8)

3.4. Determining *ex vivo* protein activity

3.4.1. Overview

In order to effectively utilize PhyB and PIF6 and a dynamic crosslink, the protein activity *ex vivo* needs to be confirmed. In current literature such as Levskaya et al. [63], the proteins have only been utilized within the context of a biological host – meaning that the proteins have not been tested outside a physiologically stable and contained unit. Because the conditions of accurate and correct protein folding can be a delicate and often a narrow window of conditions, the activity of the proteins must be tested before utilization within a hydrogel.

3.4.2. Förster resonance energy transfer (FRET)

One common way to monitor protein interaction is through Förster resonance energy transfer (FRET) which utilizes the emission of one donor fluorescent protein to excite a secondary acceptor fluorescent protein when placed in proximity to one another. The efficiency of the transfer is inversely proportional to the sixth power of distance. This sensitivity to distance makes FRET an ideal method for determining protein association. Two common FRET pairings are CFP/ YFP and mCherry/GFP. Because the mCherry emission is close to that of the association wavelength of PhyB and PIF6, CFP and YFP were chosen as the FRET pair. PhyB was conjugated to CFP and PIF6 was conjugated to YFP, both via golden gate cloning.

To measure the relative FRET, the excitation wavelength was set to the peak of CFP (430 nm) and the relative emission at CFP (480 nm) and YFP (535 nm) were measured. For this experiment relative FRET was determined by the equation below:

$$Relative\ FRET = \frac{Absorbance_{532\ nm}}{Absorbance_{474\ nm} + Absorbance_{532\ nm}}$$

a)

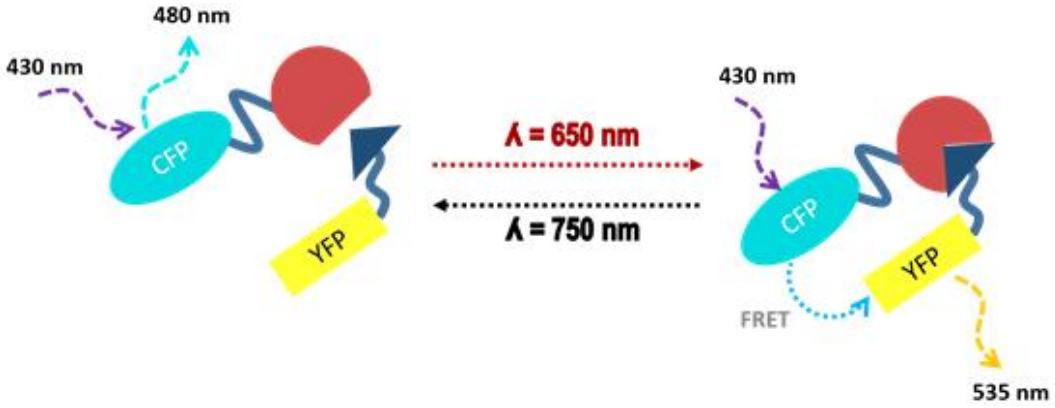

b)

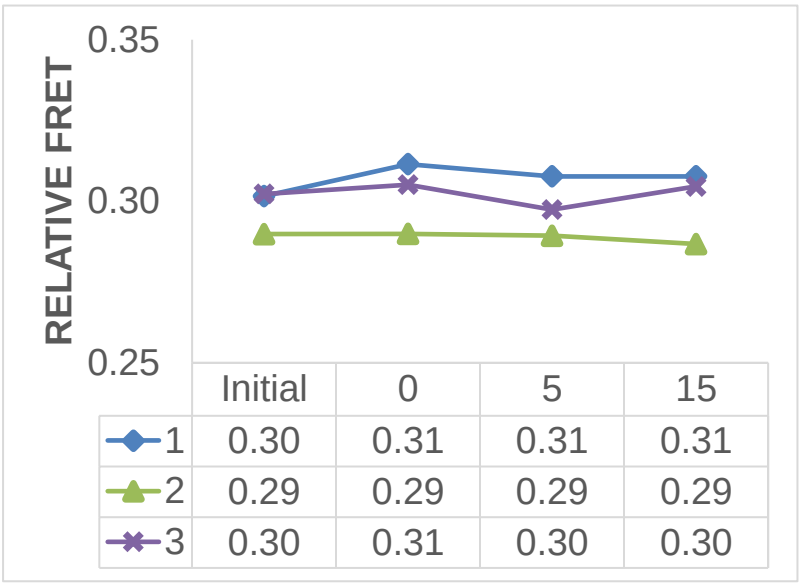

	Initial	0	5	15
1	0.30	0.31	0.31	0.31
2	0.29	0.29	0.29	0.29
3	0.30	0.31	0.30	0.30

Figure 9. FRET to measure PhyB and PIF6 interactions.

PhyB and PIF6 interaction brings CFP and YFP into a proximal distance, enabling FRET. As shown in (a) excitation at 430 nm would results in 480 nm emission without FRET and 535 nm emission if FRET occurs. FRET analysis of protein association is determined via a relative emission. Relative emission showed minimal changes when exposed to 650 nm light for 15 minutes (b) suggesting FRET is not an efficient method to determining protein activity. The FRET signal may have been drowned out by the background noise or been too weak based on sub-optimal orientation of the fluorescent proteins. Fluorescence measurements were taken upon 430 nm excitation through a Tecan M1000 Pro.

In the case of PhyB and PIF6, FRET was not sensitive enough to discern a difference in the fluorescence when exposed to 650 nm light for up to 15 minutes. FRET requires relatively pure samples of proteins as the background noise of the fluorescence molecules could drown out any FRET signal. If only a small percentage of the proteins

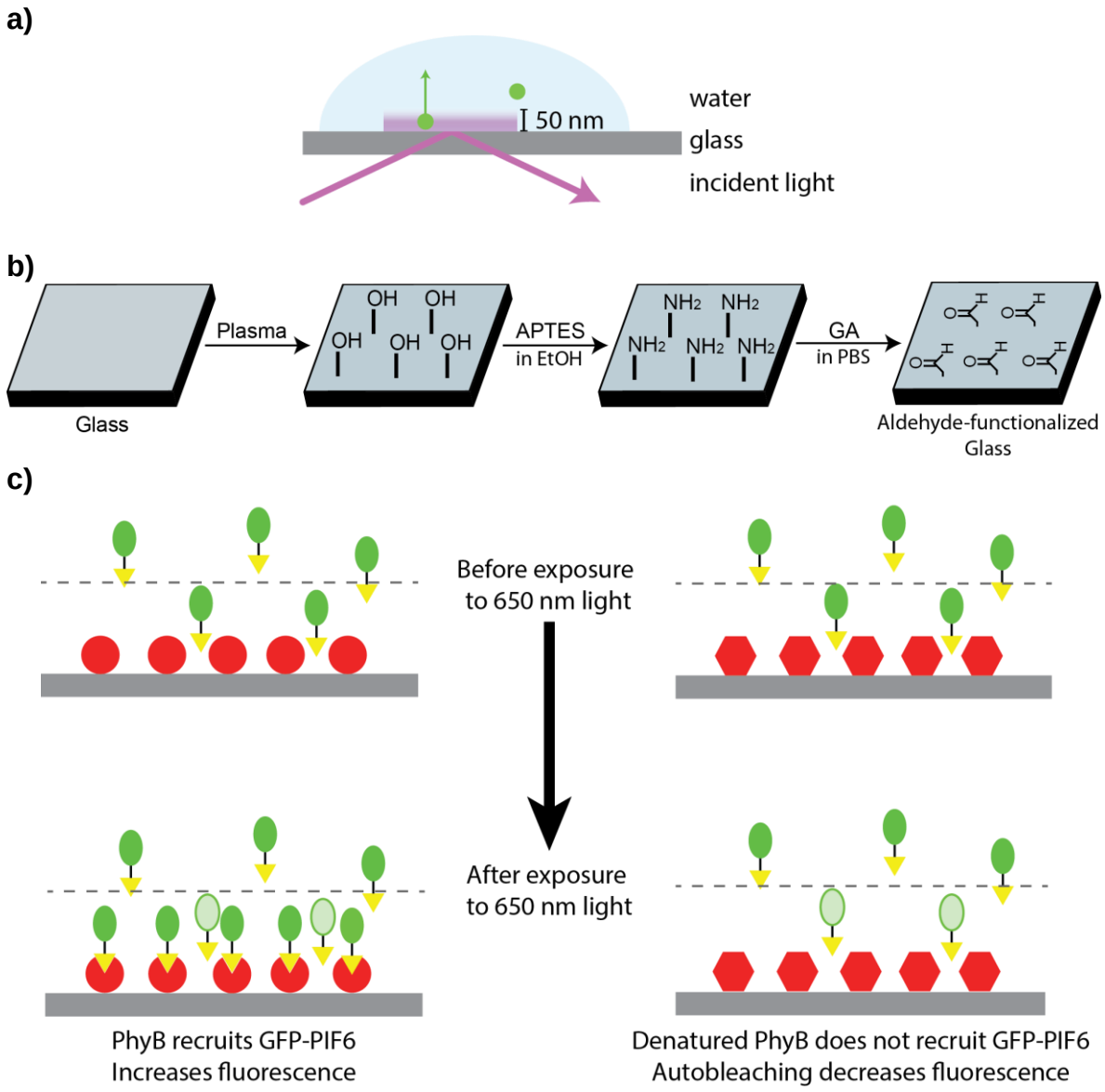

Figure 10. TIRF to measure PhyB activity *ex vivo*.

TIRF illuminates fluorophores in a limited range (~50 nm) above a glass surface as depicted in (a). Glass was functionalized with APTES and glutaraldehyde to enable protein conjugation (b). Protein activity of PhyB was tested as depicted in (c). Upon exposure to 650 nm light, PhyB recruits additional PIF6-GFP to the 50 nm range where TIRF can illuminate fluorescent proteins. Existing PIF6-GFP molecules within the 50 nm region will experience photobleaching, but recruitment of additional PIF6-GFP will result in a net increase in fluorescence. Denatured PhyB, however, will be unable to recruit PIF6-GFP and thus, only photobleaching of the existing PIF6-GFP will occur.

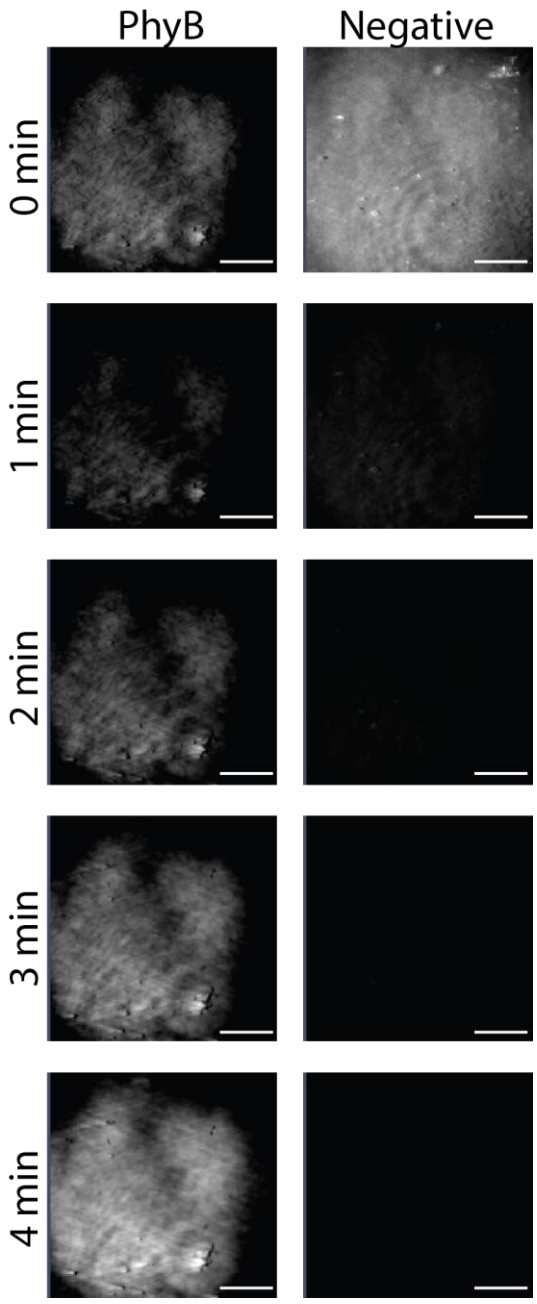

Figure 11. TIRF measurements of PhyB activity and recruitment of GFP-PIF6.

Active PhyB recruits PIF6-GFP to the surface. At one minute, some initial photobleaching of the existing PIF6-GFP can be seen. At 4 minutes, enough PIF6-GFP has been recruited to result in a net increase in fluorescence. (Left) Denatured PhyB, however, will be unable to recruit PIF6-GFP and thus, only photobleaching of the PIF6-GFP will occur. (Right) Scale bars are 10μm.

interacted with each other, the FRET signal could be too weak compared to the background noise. Additionally, FRET can be sensitive based on the orientation and distance of the fluorescent proteins. It is possible that the orientation in which the PhyB and PIF6 interact is unfavorable for FRET analysis. (Figure 9)

3.4.3. Total internal reflection fluorescence (TIRF) microscopy

Another potential method for monitoring protein association is through total internal reflection fluorescence (TIRF) microscopy. When two materials with different refractive indexes share a boundary, there is an angle at which an incident light can be completely reflected. Upon complete reflection of that incident light, an evanescent or exponentially decaying wave of power from that light will be transmitted into the second medium. TIRF microscopy utilizes the power emitted from the evanescent wave to illuminate a very tightly controlled area above an interface (around 50 nm) for fluorescence microscopy. In Levskaya et al. [63], PhyB was conjugated with a Kras domain, which allows the PhyB to embed in the plasma membrane. TIRF microscopy was then used to visualize the recruitment of PIF-

YFP to the membrane to confirm the robustness of the protein interaction.

In a similar fashion, PhyB was conjugated to a glass side and used to watch recruitment of the PIF6-GFP to the surface of the glass. To bind proteins to a glass surface, glass was functionalized to have aldehyde groups. First, glass slides were left overnight in a solution of 1M NaOH. Upon drying with nitrogen, the glass slides were exposed to oxygen plasma for 2 minutes. A solution of 2 v/v% of APTES in ethanol were added to the glass slides for 1 hour at room temperature. The glass slides were then washed with ethanol and dried on a hotplate for 1 hour at 100°C. A 2.5 v/v% solution of glutaraldehyde in phosphate-buffered saline (PBS) was exposed to the glass slides at room temperature for 30 minutes. Finally, the glass slides were dried with nitrogen and stored in a desiccator for up to 24 hours. (Figure 10)

To determine the protein activity of PhyB, TIRF was used to monitor the accumulation of a GFP-labeled PIF6 to a PhyB-coated glass surface. PhyB in a solution of 25 mM HEPES and 150 mM NaCl was exposed to aldehyde-functionalized glass for 1 hour at room temperature. These aldehyde groups are reactive to primary amines which can be found on amino acid groups such as lysine, arginine, asparagine, and glutamine. Immediately before TIRF experiments, a solution of GFP-PIF6 was placed on top of the PhyB-coated glass. Active and functional PhyB upon exposure to 650 nm light started recruiting PIF6-GFP to the glass surface resulting in an increase in fluorescence. Although some photobleaching can be seen within the first minute of recruitment, the eventual accumulation of recruited PIF6-GFP led to a net increase in fluorescence. (Figure 11, left)

For a negative control, PhyB was fixed to a glass surface and then allowed to dry out for 10 minutes. The protein denatured upon drying and was no longer active. This was used as a control to demonstrate that the increase in fluorescence observed was due to the active recruitment of PIF6-GFP by PhyB and not due to diffusion. When 650 nm light was exposed to the glass covered with denatured PhyB, GFP-PIF6 was not recruited to the surface. The GFP-PIF6 that was originally within the 50 nm range above the glass surface photobleached – leading to a decrease in fluorescence. (Figure 11, right) All measurements with TIRF were performed on a Zeiss Elyra PS.1 SIM/PALM Super-Resolution microscope.

3.5. Discussion

The ability of optogenetic proteins to shift conformation based on light cues enables their potential to serve as dynamic crosslinkers within hydrogel platforms. Being able to change material stiffness with light provides both an opportunity for patterning and overcoming mass transport limitations that other protein- and DNA-based hydrogels have faced. Of the potential protein candidates for the hydrogel platform, PhyB and PIF6 were chosen for two reasons. The first is their response to the red/far-red spectrum rather than blue light, which has been shown to cause DNA damage and have toxic effects on cells. The second reason is because their association and dissociation are stimulated at two distinct wavelengths. This allows a much more defined and controllable interaction than

other optogenetic proteins, such as Cry2, which quickly aggregates in the presence of blue light and gradually dissociates in the absence of light.

PhyB and PIF6 and their conjugated fluorophores were expressed and purified from *E. coli* cultures. After purification, these proteins were tested for their activity *ex vivo* as previous use of the proteins resided only within the context of a biological host. A common way of monitoring protein association, FRET, proved unsuccessful. One potential reason for the lack of FRET signal could stem from suboptimal orientation of the fluorophores when PhyB and PIF6 associate. Changing the FRET fluorophore pair or experimenting with linker lengths could allow for a more efficient transfer. Moreover, if the solutions of the PhyB or PIF6 contained many free-floating fluorophore impurities, the increased background noise could have led to a loss of signal. Although FRET proved unsuccessful, TIRF microscopy was successfully used to determine protein activity. TIRF microscopy was able to monitor the recruitment of GFP-PIF6 proteins to the surface of a PhyB-functionalized glass slide. For next steps, other protein association characterizations such as isothermal titration calorimetry (ITC) could be used to more accurately measure binding affinities and kinetics of PhyB with PIF6.

Proving these proteins are successful outside the context of a biological host was key before utilizing these proteins as a light-inducible crosslinker. Future work should also include increasing the production and purity of the PhyB. While the size of PIF6 was relatively small, the PhyB was difficult to fabricate within *E. coli* which does not easily create larger proteins. Potentially utilizing other truncated versions of PhyB (1-450, 1-624) or other co-factors such as phytochromobilin (PΦB) could prove more efficient yields, although their activity *ex vivo* would also need to be tested. In a recent paper by Burgie et al. [70], the incorporation of PΦB rather than PCB allowed for a much quicker and more stable transition to the Pfr state. Additionally, the study showed that PhyB (1-908) fragments had a high tendency to form dimers, which suggests that perhaps other truncated versions of PhyB may be more well suited for higher yields during protein purification.

Chapter 4. Hyaluronic Acid Polymer Modification and Protein Conjugation

4.1. Introduction

4.1.1. Hyaluronic acid polymers

Hyaluronic acid (HyA) is a naturally occurring linear polysaccharide polymer within our bodies, is found in the extracellular matrix of cartilage tissue, and is a vital part of multiple important processes such as wound healing and cellular signaling. Different lengths of HyA has been shown to create different immunological effects, with shorter strands causing inflammatory, immune-stimulatory, and angiogenic responses and with larger strands creating space-filling, anti-angiogenic, and anti-inflammatory effects. [71] Furthermore, HyA polymers, upon modification, are capable of a diverse range of protein patterning and microstructure formations, although it has limited ability for protein adsorption natively. [72] Because of its relative ease for protein modifications, natural degradation properties, and diverse range of tunable material properties such as mesh size, HyA has become the focus of multiple potential biomedical applications including tissue engineering scaffolding. [73]

A demonstration of the potential of HyA in biomedical applications is the ability of HyA polymers to maintain cell cultures for sensitive cell lines, including human embryonic stem cells (hESCs). Generally, hESCs are cultured on mouse embryonic feeder layers (MEFs) or on mouse extracellular matrices such as Matrigel to maintain pluripotency. For differentiation, hESCs are transported to other mediums for differentiation which creates a large break and rapid transition between proliferation and differentiation conditions. In Gerecht et al. [74], HyA polymers were utilized as a scaffold to create an environment that would transition from proliferation to differentiation conditions seamlessly with no animal derived products.

HyA polymer's ability to be modified for protein conjugation makes it a particularly favorable candidate for both downstream studies and integration into this dissertation's platform. The polysaccharide generally is modified at the carboxylic group and occasionally at the primary alcohol to have reactive groups that have either or both crosslinking and protein conjugation abilities. [75-83] The ability to modify HyA polymers without compromising cell culturing conditions have led to novel tissue engineering materials, including one "smart" hydrogel for adipose tissue engineering that initiates crosslinking based on a thermo-responsive radical initiator which was conjugated covalently to the HyA polymer. [84]

One common way for modifying HyA includes the use of *N*-(3-dimethyl-propyl)-*N*-ethylcarbodiimide hydrochloride (EDC) as a catalyst to prime the carboxylic group to react with either *N*-hydroxysulfosuccimide sodium salt (sulfo-NHS) [85] or 1-hydroxybenzotriazole (HOBt) [86]. However, many studies choose to modify HyA with methacrylate groups through methacrylate anhydride or glycidyl methacrylate because methacrylate groups can react with nucleophiles such as primary amines and thiols while

also participating in crosslinking chemistries through radical polymerization. [87-92] For this dissertation, HyA was chosen as the base polymer because it is bio-inert, and able to sustain both protein conjugation and crosslinking chemistries necessary to create the dynamic stiffness hydrogel platform.

4.1.2. Click chemistry as a method for protein conjugation

For the proposed platform, any products or reagents that modify the HyA polymers should either be dialyzable or be active at physiological conditions. There are a variety of bio-inert chemical reactions, categorized as click chemistries, that can occur near physiological conditions with respect to pH, salinity, and temperature, making them ideal for downstream biological studies and environmentally-sensitive proteins. The yield, specificity, and the biologically innocuous conditions make it a prime choice for hydrogel modifications or crosslinking. [93] It should be noted that not all click chemistries are appropriate for all applications as some require catalysts such as copper or triethylamine (TEA) which could be toxic themselves or create toxic side products. [94]

Specifically, there are reactions under the umbrella of click chemistry that have been deemed “pseudo-click” which maintains mild reaction conditions, high reactivity, and high yield. However, these reactions may have some limitations with biorthogonality, which is the ability for a chemical reaction to occur without interrupting biological native processes. [93] Among the pseudo-click chemistries, the thiol-ene reaction has been utilized for both hydrogel formation [95] and protein conjugation [96]. While this reaction has been well characterized to be efficient with the use of photoinitiators, this reaction has also been documented to also be efficient under mild basic catalytic conditions. [97] Specifically, the addition of a thiol to the electron deficient double bond in acrylate and methacrylate group is characterized as Michael-addition chemistry which is the addition of a nucleophile to the β-carbon on an α, β-unsaturated carbonyl group. Because of the stabilization due to the double bonded oxygen, nucleophilic attacks on electron rich double bonds become more favorable.

For implementation into the hydrogel platform, proteins were modified to have exposed thiol groups. There are a variety of chemistries that will modify primary amines on the surface of proteins into thiol groups, including 2-iminothiolane (Traut’s reagent) which requires mild reaction conditions. In this dissertation, the hydrogel platform utilizes the reaction of thiols with methacrylate groups for protein conjugation. Although this reaction suffers from lower reactivity than its acrylate or vinyl sulfone counterparts, it was chosen because it was known to be more stable and less likely to suffer hydrolytic degradation. [98]

4.2. Materials

Sodium Hyaluronate was purchased from Lifecore (Chaska, MN). Glycidyl methacrylate, triethylamine (TEA), isopropanol, deuterium oxide, dimethylformamide (DMF) and Hystem-C™ kits were purchased from Sigma-Aldrich (St. Louis, MO) Traut’s Reagent and sodium hydroxide (NaOH) were purchased from ThermoFisher Scientific

(Waltham, MA). Additionally, the probes used for RT-PCR for PPARG, Myo-G, and RUNX2 expression were purchased from ThermoFisher Scientific. Phosphate-buffered saline was purchased from Life Technologies (Carlsbad, CA) Ethylenediamine tetraacetic acid (EDTA) and hydrochloric acid were purchased from VWR (Radnor, PA).

4.3. Method: Hydrogel platform formation

4.3.1. Creating methacrylated hyaluronic acid (MHyA) polymer strands

Methacrylated hyaluronic acid (MHyA) has the potential for radical polymerization and protein conjugation through click chemistry. HyA polymers were modified via a protocol found in Bencherif et al. [99] to have methacrylate groups for protein conjugation. Sodium hyaluronate was purchased from Lifecore in powder form of various lengths and dissolved in a 50:50 mixture of PBS:DMF solution at room temperature with gentle shaking for 2 hours. Triethylamine (TEA) was added to create an excess base environment and allowed to dissolve for 30 minutes at room temperature on the shaker. Glycidyl methacrylate (GM) was added in various ratios according to Table 2. After reacting the solution between 5-10 days, the solution was precipitated with isopropanol. The solution was centrifuged, resuspended in deionized water, and then dialyzed with deionized (DI) water for 3 days. Finally, the MHyA was lyophilized to create a final product. Table 2 contains a summary of reaction conditions and the resulting degrees of methacrylation which were measured via proton nuclear magnetic resonance spectroscopy.

Length of Polymer	GM:HYA Molar Ratio	Days Reaction	Degrees of Methacrylation
1500 kDa	150:1	5 days	1%
1500 kDa	175:1	5 days	5%
1500 kDa	200:1	5 days	10%
60 kDa	100:1	5 days	7%
60 kDa	100:1	10 days	7%
60 kDa	600:1	5 days	11%
60 kDa	800:1	5 days	15%-22%**

Table 2. Summary of resulting degrees of methacrylation on HyA polymers from various reaction conditions.

4.3.2. Characterization of MHyA via ^{1}H NMR spectroscopy

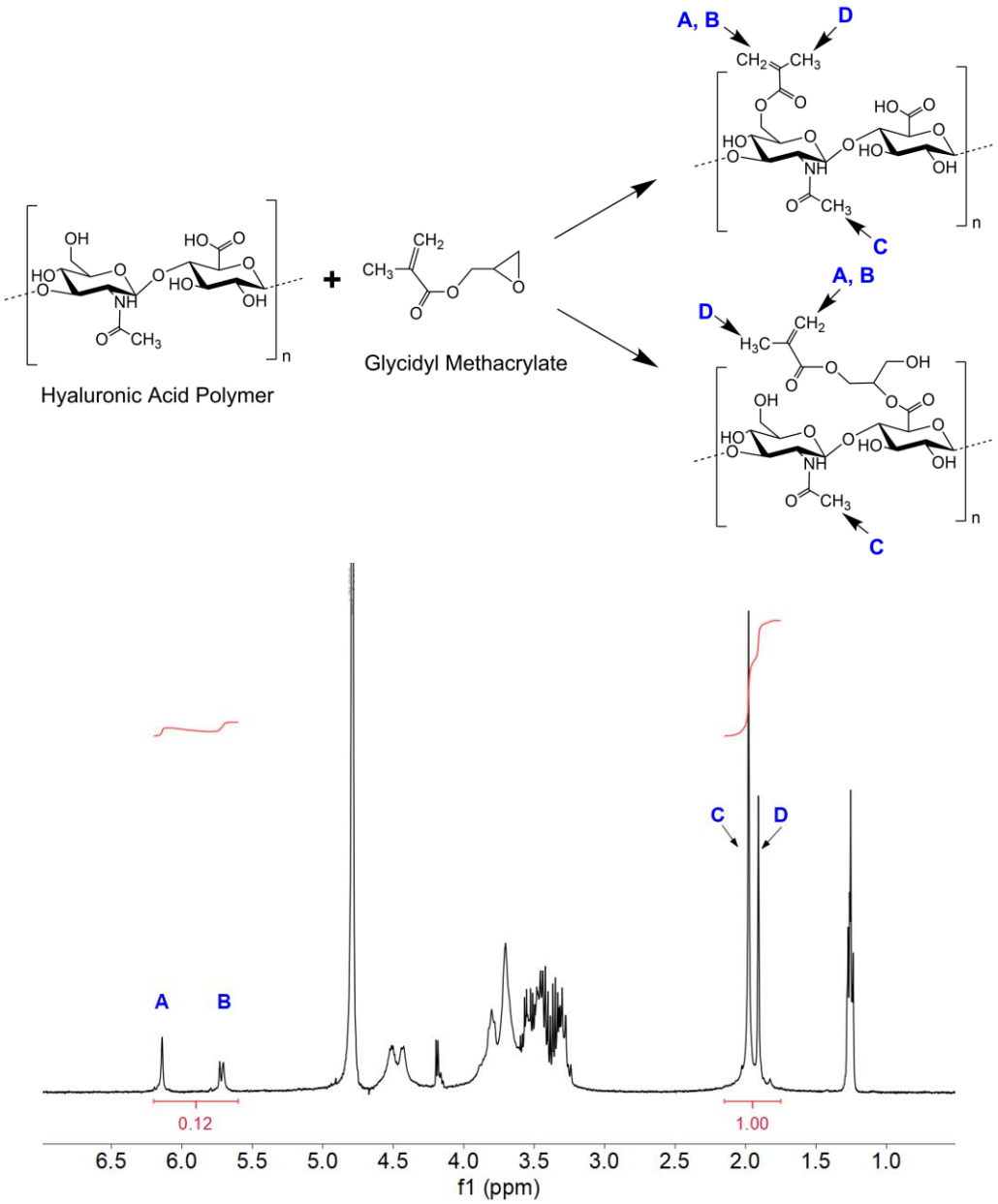

Figure 12. Example ^{1}H NMR for determining degrees of methacrylation on HyA.

The top shows the reaction of the glycidyl methacrylate with the HyA polymer. The bottom is an example NMR that shows an approximate degree of methacrylation of 12%. NMR peaks to corresponding protons are indicated with letters.

The protocol for the modification of the HyA polymers was optimized and confirmed via high-resolution proton nuclear magnetic resonance (^{1}H NMR) spectroscopy on a

Bruker Advance 400 console with Oxford Instruments 9.4 T magnet. MHyA polymers were dissolved between 0.5-1.0 wt% solutions with deuterium oxide (D_2O) as a solvent. Samples were taken at room temperature for 32 scans. The degrees of methacrylation (DM), which is the percentage of HyA disaccharide units with a methacryloyl group, is based on the relative peaks on the NMR spectra. For consistency, all spectra were shifted to the base D_2O solution. The HyA methyl protons were used as the reference and are found and integrated from 1.75-2.15 ppm with a peak around 1.9 ppm. The methacrylate protons were found and integrated from 5.6-6.2 ppm with peaks at 5.6 and 6.1. An example NMR can be found in Figure 12.

4.3.3. Thiolation of proteins for click chemistry conjugation to HyA and MHyA

Proteins were primed for conjugation by creating thiol groups from primary amines found on the surface of the protein. These thiols were reacted with the methacrylate groups on the HyA polymer strands via thiol-ene click chemistry. Traut's reagent (2-iminothiolane) was purchase from Pierce Thermo-Fischer Scientific and was used to convert primary amines such as those found on the side groups of arginine, lysine, and histidine, into sulfhydryl groups. Traut's reagent was resuspended in PBS-EDTA buffer (PBS buffer with 2-5 mM EDTA and adjusted to a pH = 8.0) to a concentration of 100 mM and allowed to react to the proteins in 20-50 times molar excess. Because Traut's Reagent will kinetically prefer to react with primary amines (~5 minutes half-life) over hydrolysis (~1 hour half-life), the proteins were incubated with Traut's Reagent for one hour at room temperature before proceeding to future steps.

4.3.4. Hystem-C™ hydrogel network formation

Hystem-C™ kits were purchased from ESI BIO which comes with thiol-modified sodium hyaluronate (Glycosil®, 10 mg), thiol-modified gelatin (Gelin-S®, 10 mg), Extralink® (polyethylene-diacrylate/PEGDA, 5 mg), and degassed water. After allowing the individual components to stabilize at room temperature, the degassed water was added to the Glycosil® and Gelin-S® and allowed to dissolve on the shaker at room temperature for 1 hour.

To make a semi-IPN network, the free strand was created separately. MHyA was dissolved in PBS-EDTA buffer and allowed to dissolve for 1 hour at room temperature on the shaker. Thiol-modified PhyB and PIF6 were then added and allowed to react with the MHyA on the shaker for an additional 1 hour at room temperature to create the free strand.

The free strand, additional thiol-modified PhyB and PIF6 proteins, Glycosil® and Gelin-S® were mixed together. Extralink® was introduced last and mixed thoroughly into the solution. Then final solution was set and allowed to gel at room temperature for 30 minutes. The hydrogels were then incubated at room temperature to swell overnight in PBS before imaging or analysis via atomic force microscopy (AFM).

4.4. Hyaluronic acid hydrogels stiffness range and cell culture capabilities

4.4.1. Testing protein conjugation to the Hystem-C™ hydrogel network

Protein conjugation to the Hystem-C™ hydrogel was tested via mCherry proteins. After the mCherry proteins were reaction with Traut's reagent, the protein was mix into the Hystem-C™ hydrogel. The Extralink®, which binds the thiol-modified gelatin to the thiol-modified HyA polymers, was used to also bind the thiol-modified mCherry proteins to the thiol-modified HyA polymers. The final concentration of the gels was made to be 0.4 wt% Glycosil®, 0.4 wt% Gelin-S®, 0.4 wt% Extralink® and with a final concentration of 0.2 mg/mL of thiol-modified mCherry proteins.

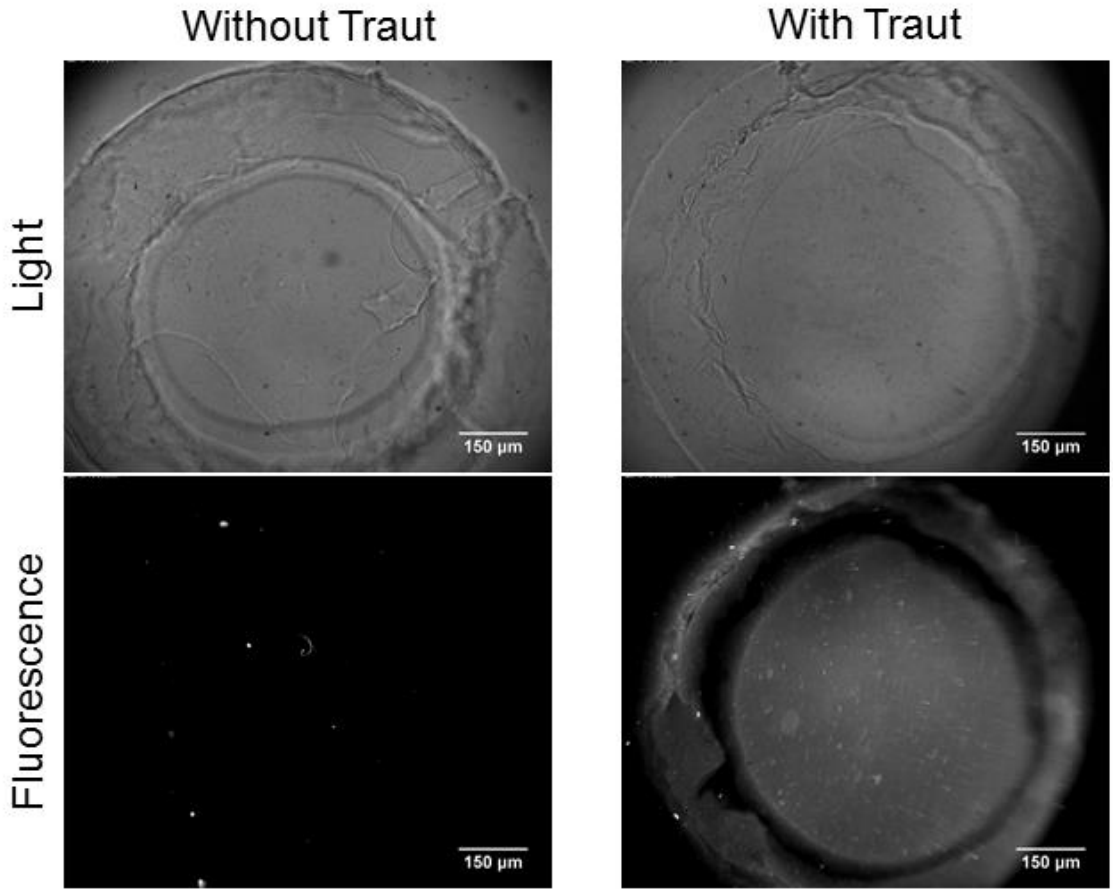

Figure 13. Hystem-C™ hydrogel conjugation with mCherry.

Protein mCherry was modified by Traut's Reagent and then added to the hydrogel mixture before gelation. The bright field images (top) and the fluorescent images (bottom) of the hydrogels were taken after 72 hours of incubation with PBS. The images were taken with the same exposure time and subjected to the same modifications. Scale bars are 150 µm.

Following gelation, the hydrogel was incubated with PBS over a period of 72 hours to ensure that the conjugation was covalent and to prevent non-specific binding. Every 24 hours, the PBS was discarded and replaced to remove unbound mCherry proteins. Additionally, mCherry proteins that had not been modified by Traut's reagent were added to a separate hydrogel and used to compare for non-specific fluorescent protein retention. This hydrogel was used to set the background fluorescence during image processing. After 72 hours, fluorescence imaging confirmed that the Hystem-C^{TM} hydrogel was capable of protein conjugation only after proteins were exposed to Traut's reagent. (Figure 13)

Similarly, a semi-interpenetrating polymer network (semi-IPN) hydrogel was made with the Hystem-C^{TM} network as a base and a MHyA free polymer strand. This platform was created and conjugated to PhyB-mTurquoise and YFP-PIF6. The hydrogel was incubated in PBS over a period of 72 hours to ensure that the conjugation was covalent and to prevent non-specific binding. Every 24 hours, the PBS was discarded and replaced to remove unbound proteins. Confocal microscopy confirmed the covalent conjugation of proteins into the hydrogel platform. (Figure 14)

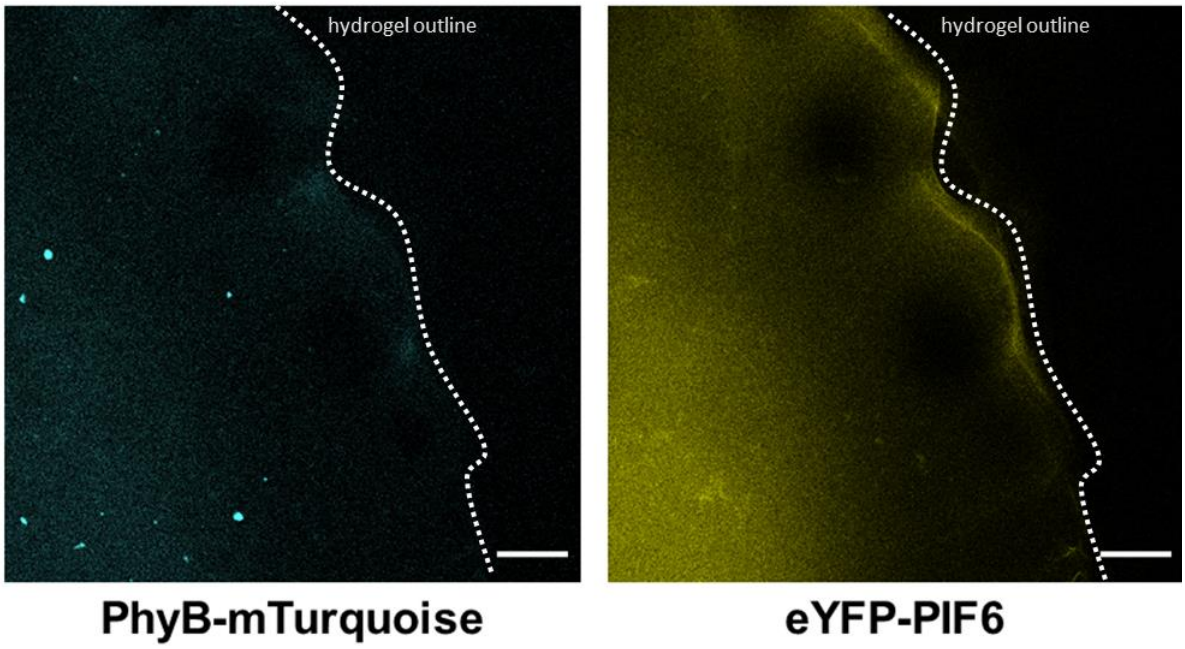

Figure 14. Confocal microscopy image of Hystem-C^{TM} platform with conjugated PhyB-mTurquoise and eYFP-PIF6.

Fluorescence of the PhyB and PIF6 can be seen to follow the outline of the hydrogel depicted by the white dotted line. Scale bars are 200 µm.

4.4.2. Testing the stiffness range Hystem-C^{TM} hydrogels

Characterization of the Hystem-C^{TM} hydrogels' bulk stiffness were made via the AFM. The components of the Hystem-C were varied in their weight percentages (Figure

15). The range of stiffness of the Hystem-C™ ranged from 0.2-16 kPa. As expected, the stiffness increase non-linearly with respect to polymer and crosslinker concentration (Extralink®). This data suggests that the hydrogel platform is capable of a wide range stiffness magnitudes for cell culture studies.

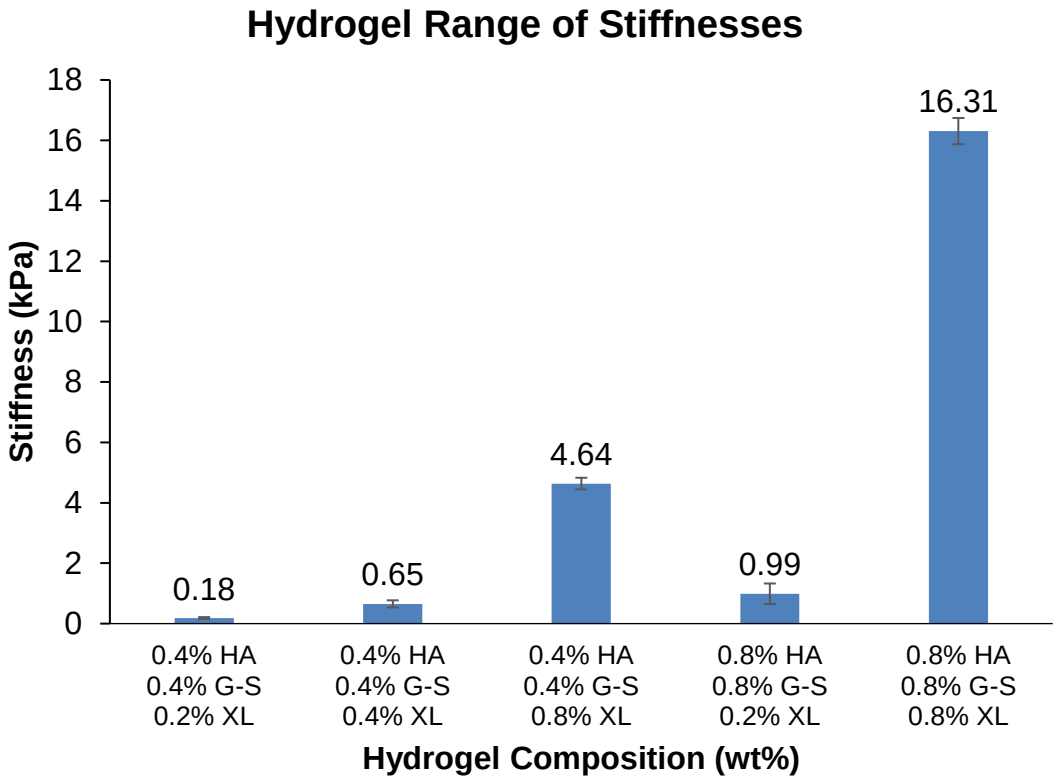

Figure 15. AFM measurements of Hystem-C™ gel stiffness with various concentrations of the components.

HA stands for Glycosil® which is a thiol-modified hyaluron; G-S stands for Gelin-S® which a thiol-modified denatured collagen; and XL stands for Extralink® which is a thio-reactive crosslink, PEGDA. Error bars, ± SD (n=100 over a single hydrogel)

4.4.3. Culturing hMSCs in different stiffness hyaluronic acid gels

The Hystem-C™ system was made into two different stiffnesses (~200 Pa and ~4-5 kPa) and used to culture hMSCs at a concentration of 10^6/mL for 6 days. The cells were cultured in maintenance media and were not exposed to any differentiating factors. Preliminary cultures of hMSCs on the Hystem-C™ hydrogels showed morphological differences within the first 24 hours of culture and were harvested after 6 days. (Figure 16)

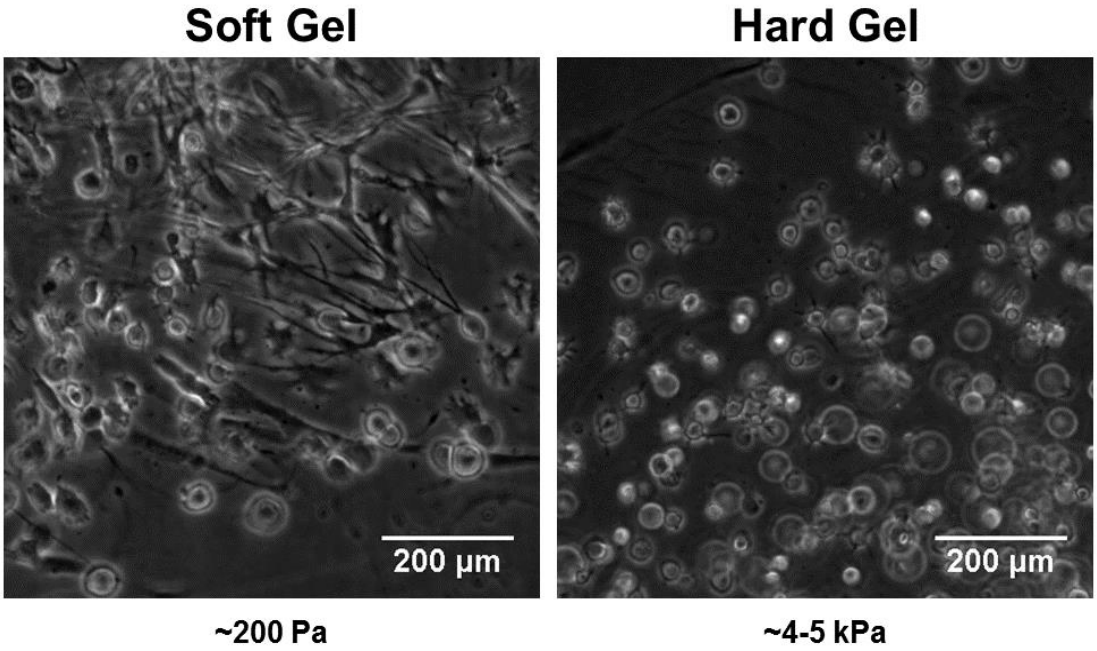

Figure 16. Phase contrast images of hMSCs in Hystem-C™ hydrogels after 6 days of culture in non-differentiating media.

The cultures were then harvested for analysis via quantitative reverse transcription polymerase chain reaction (qRT-PCR). An adipogenic marker, PPARG, myogenic marker, MYO-G, and an osteogenic marker, RUNX2, were used to quantify the differentiation of the hMSCs. There was no significant data of MYO-G expression in either condition. However, there was a significant amount of RUNX2 expression over that of PPARG, which indicates that both gels induced osteogenic lineages (Figure 17a). Immunofluorescence was used to visualize the expression of RUNX2 and PPARG expression within the cells (Figure 17b). Cells cultured on softer gels showed an increased expression of the adipogenic marker as compared to cells cultured on the harder gels. Interestingly, there also seems to be an apparent increase in RUNX2 expression in the cells cultured on the softer gel as well.

While the gels were made with a height of around 1000 µm, it is possible that the stiffness of plastic on which the gels were formed caused the cells to experience a much stiffer matrix than the stiffness of the hydrogel itself. Because plastic can range from 100 to 1000 times the stiffness of either hydrogel, the cells in the softer gel could differentiated into osteoblasts because of the inherent and apparent stiffness of the plastic dish. Additionally, the hMSCs were cultured on hard plastic for a week before being transplanted into the hydrogel. From evidence in Yang et al. [15], there is a chance that the hMSCs were already exposed for too long to the tissue culture plates, had “memory” of those culturing conditions, and had already committed to the osteogenic lineage.

a)

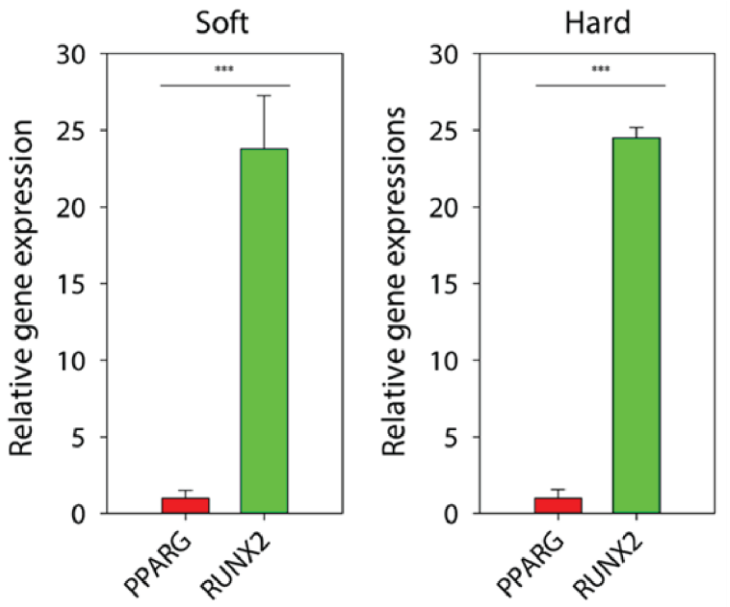

b)

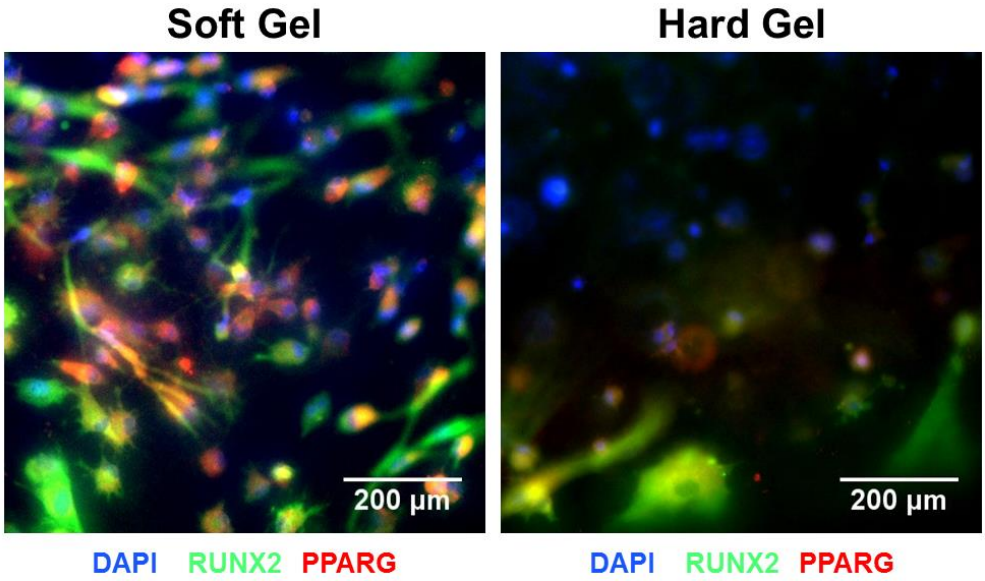

Figure 17. Differentiation markers of hMSCs in Hystem-C hydrogels after 6 days of culture in non-differentiating media.

The softer gel had a stiffness of ~200 Pa and the harder gel was around ~4-5 kPa. (a) Levels of mRNA for the PPARG (red bars) and RUNX2 (green bars) in the softer and the harder condition were normalized to those of GAPDH and were acquired on day 6 of culture. Error bars, ***P<0.001, ± SD (n=4), (b) Immunofluorescence showing expression of the PPARG and RUNX2 (red, PPARG; green, RUNX2; blue, nuclei), Scale bars, 200 µm.

4.5. Discussion

Hyaluronic acid hydrogels were chosen for this platform because it has both the ability to culture sensitive cell lines such as hESCs and to be modified for a variety of protein conjugation or crosslinking chemistries. Additionally, hyaluronic acid hydrogels have the added benefit of being transparent. Because the platform relies on light cues, permeation of the light source will enable downstream applications where patterning may become applicable.

In this chapter, the hyaluronic acid hydrogels were successfully modified to have methacrylate groups to enable protein conjugation. By transforming surface primary amines on proteins into thiols, proteins were covalently added to the methacrylate groups on the hyaluronic acid polymer strands through click chemistry. This thiol-ene reaction is bio-inert with high yields and efficiencies. Additionally, these chemistries do not require the use of toxic catalysts and can maintain physiological conditions, making it ideal for downstream cell culturing applications.

NMR spectroscopy confirmed and quantified the degree of methacrylation of the hyaluronic polymer strands, and confocal and fluorescence microscopy were used to visualize the successful thiol modification of proteins and its conjugation to the hydrogel platform. The hyaluronic acid hydrogels also demonstrated a large range of stiffnesses by altering the weight percentage of the polymer strands and crosslinker. Furthermore, the cell culturing capabilities of the platform was verified through long-term cell cultures of hMSCs. These hMSCs were cultured in different stiffness hydrogels and expressed unique morphological phenotypes in each condition. Although the qRT-PCR data showed that the two cultures had similar relative expression levels of osteogenic differentiation markers, immunofluorescence showed that the softer gel hMSCs expressed more adipogenic markers than the harder gel.

For future work, other methods of HyA modifications could be explored to increase the efficiency of protein conjugation. Some common click chemistries to consider include vinyl sulfone or sulfo-NHS/EDC which are compatible with HyA polymers. Additionally, the hydrogel platform discussed in this dissertation requires the incorporation of a free strand. While for this dissertation, the free strand was created with hyaluronic acid polymers, creating a blended hydrogel with different polymer strands could prove to be more efficient or tunable. For instance, polyethylene glycol (PEG) could also be used as a potential alternative polymer for the base polymer or free strand. PEG hydrogels are also able to form transparent, stiffness-tunable hydrogels [91] and can support proteins conjugation chemistries [101].

Chapter 5. Atomic Force Microscopy of the Hydrogel Platform

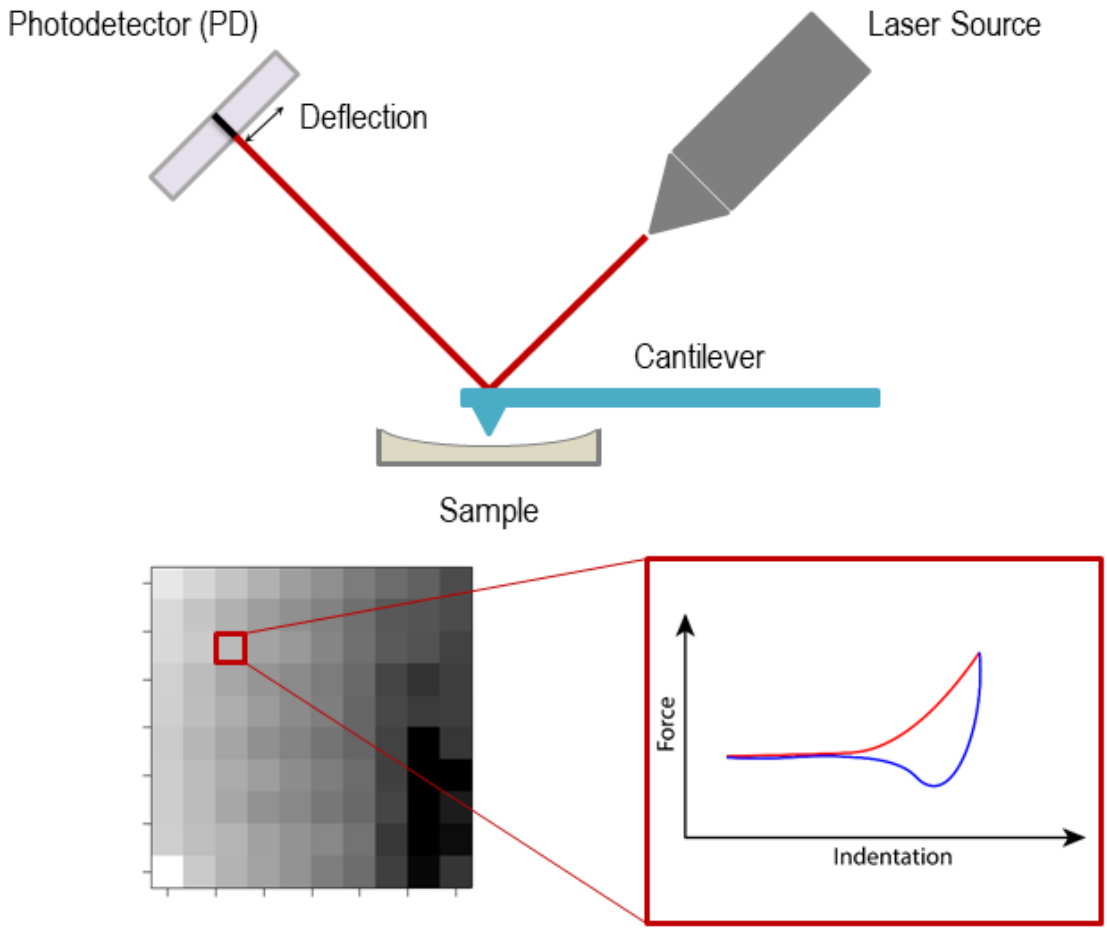

Figure 18. Schematic of atomic force microscopy (AFM) to measure the stiffness of a sample.

A laser source is focused on the tip of a cantilever and reflected onto a photodetector. As the cantilever is lowered into and removed from the sample, the cantilever will bend, and the deflection of the laser source will determine the degree to which the cantilever is bent. The AFM will then take measurements to form a grid of force vs. indentation curves which will translate into elasticity measurements.

5.1. Introduction

5.1.1. Atomic force microscopy (AFM)

There are a variety of measuring devices that could be used to determine the material properties of the proposed HyA hydrogel platform. One common way is using a machine called a rheometer, which utilizes applied stresses to measure the response of the material. The data measured is then used to determine the material properties such as the storage and loss modulus. [102-104] Increasingly, atomic force microscopy (AFM) has become a popular way to measure the stiffness of soft biological materials because of its ability to determine elasticity with high spatial resolution rather than just bulk measurements. [105] While the AFM is well known to characterize very stiff materials, the AFM is simultaneously capable of measuring very delicate samples such as tissues or single cells with a great degree of accuracy. [106-109]

In most linear materials, the Young's modulus, E, will be constant, but in non-linear materials the elasticity will be a function of the strain. For example, the relationship between the stress (σ) and strain (ε) curve will relate linearly by the Young's modulus through Hooke's law (σ=Eε) for linear elastic solid substances such as rubber, steel, and bone. Newtonian fluids, such as blood plasma, follow a different law (σ=μ·dε/dt) where the stress is proportional to the rate of strain by a property called viscosity (μ). Viscoelastic materials, such as cells or hydrogels which exhibit characteristics of both solids and liquids, have a nonlinear relationship between the stress and strain. Because biological materials, cells, and the extracellular matrix are non-linear viscoelastic materials, a sensitive, precise method of determining elasticity is necessary.

Material properties of these viscoelastic samples are measured based on the theory of Hertz which relates the elasticity of two bodies. [110] By fitting to the Hertzian mathematical relationship, one can determine Young's Modulus, or elasticity, of a given sample. The AFM utilizes the Hertz theory, relates the relative elasticities of the cantilever to the measured sample, and fits for the elasticity of the sample. [111] Multiple papers have demonstrated that contact AFM can be utilized to accurately determine the elasticity of polymers utilizing either spherical [112] or conical tips [113]. For soft or viscoelastic materials where a cone (or spherical) shaped cantilever tip is used, the Hertz theory is modified via the Sneddon model which assumes a cone-shaped indenter. [114] Based on a cone geometry, the relationship between the force applied and indentation distance are as follows:

$$Force = \frac{2}{\pi}\frac{E}{(1-\upsilon^2)}\tan(\alpha)\,D^2$$

The constant α is the semivertical (opening) angle of the cone tip and D represents the indentation distance. The Poisson ratio, υ, is generally approximated to 0.5, and is typical for water, cells, and incompressible materials. Thus, the equation simplifies to:

$$Force = \frac{8}{3\pi}E\tan(\alpha)\,D^2$$

It should be noted that the cantilever used in this dissertation was of a pyramidal shape [115] which, based on the Hertz model and assuming a Poisson ratio of 0.5, would simplify to:

$$Force = \frac{2\sqrt{2}}{3} E \tan(\alpha) D^2$$

However, lines of fit were simplified by utilizing the existing MFP3D's fitting program's calculations which could only approximate only to a cone shape. Because the coefficient difference is roughly a 10% difference, fits to a cone were considered sufficiently accurate for determining the elasticity of the hydrogels measured.

5.1.2. Semi-interpenetrating polymer networks (Semi-IPNs)

Hydrogel networks consist of polymer strands that are connected to each other via chemical or physical crosslinks to form a network. Introducing a free polymer strand that is not bound covalently to that crosslinked network creates a semi-interpenetrated polymer network (semi-IPN). These types of hydrogel networks have gained interest in the field of drug delivery and tissue engineering scaffolding as a novel way to create complex and potentially more stable structures. [116-118] In the case of the proposed platform, my hydrogel platform has two components: the free strand and the base polymer network. The base polymer network sets an established hydrogel network which already has an inherent stiffness and material properties. A free strand is incorporated into the established network of hydrogel polymers during hydrogel formation to create the semi-IPN structure.

5.2. Materials

Irgacure 2959 was purchased from BASF Corporation (Southfield, MI). Acetic acid was purchased from Spectrum Chemicals (New Brunswick, NJ). 3-(Trimethoxysilyl) propyl methacrylate and 2-ethanesulfonic acid (MES) were purchased from Sigma-Aldrich (St. Louis, MO). Ethanol was purchased from Decon Laboratories (King of Prussia, PA). Phosphate-buffered saline was purchased from Life Technologies (Carlsbad, CA). Cantilever tips TR400PB were purchased from Oxford Instruments (Abingdon, United Kingdom). Sulfo-NHS (N-hydroxysulfosuccinimi) and EDC (1-Ethyl-3-(3-dimethylaminopropyl) carbodiimide) were purchased from ThermoFisher Scientific (Waltham, MA).

5.3. Methods

5.3.1. AFM set up

The AFM head is the MFP-3D model from Oxford Instruments and the cantilevers were purchased from the same company with catalogue number TR400PB which were

recommended for use on biological samples. The cantilever tips were calibrated against a glass surface before all experiments. To accurately determine elasticity, the AFM requires precise calibrations of the cantilever before any measurement of samples can be taken. Force maps were taken on the hydrogel platform such that the same area was measured over the course of any experiment. A schematic of the AFM and a force map can be seen in Figure 18. Before any measurements, the hydrogel platforms were incubated in PBS for over 24 hours to ensure that the hydrogels are in their final state after swelling. Furthermore, the gels were exposed to no shorter than 1 hour of 750 nm light before performing the initial stiffness calculations. With an AFM, the elasticity of the material was determined through the Hertzian equation, which relates the relative elasticity of the cantilever and the sample measured.

Force curves from AFMs have multiple distinct characteristics. As shown in Figure 19, the cantilever bends at multiple stages of the force indentation curve. Before entering the sample, the cantilever remains straight and unbent. The cantilever begins bending as it interacts with the sample, causing the deflection to increase. During the retraction of the cantilever from the sample, the adhesive forces from the sample may cause the cantilever to bend into a convex shape, creating a characteristic spike in the force curve. When the cantilever is raised sufficiently to counteract the adhesive forces, the cantilever returns to its originally unbent shape. The part of the force curve from when the cantilever is lowered

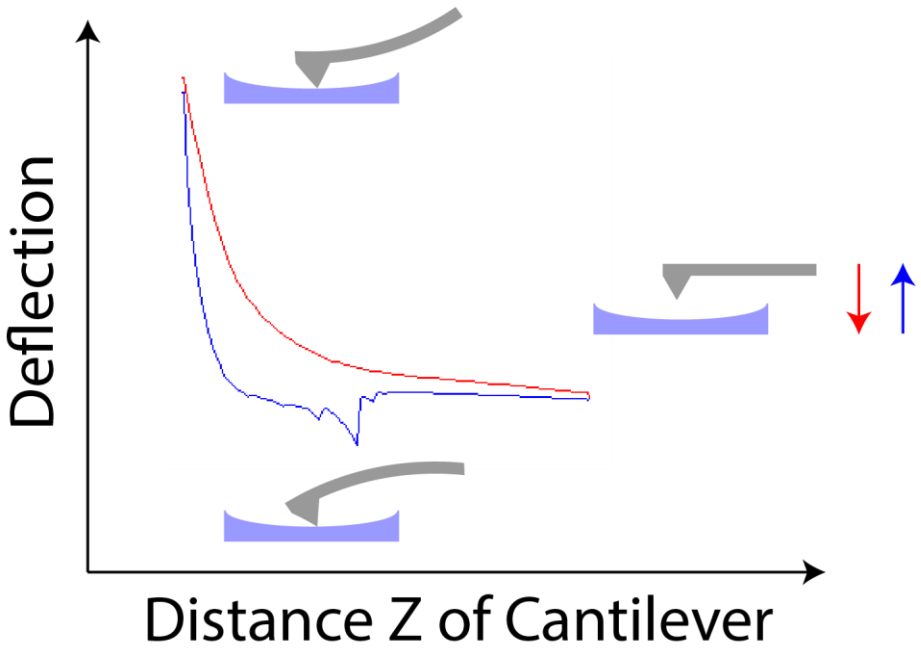

Figure 19. Force curves of AFM on hydrogel surfaces.

The red line depicts the deflection curve as the cantilever is lowered into the sample and the blue line depicts the deflection curve as the cantilever is retracted from the sample. As the cantilever is lowered into the sample, the cantilever bends increasing the deflection. After hitting a trigger deflection point set by the instrument, the cantilever is retracted. As the cantilever retracts, the adhesion forces will cause the cantilever to deflect past its resting state, resulting in certain “spikes” that can be translated into adhesive data of the hydrogel.

into the sample is fitted to the Hertz model. The retraction can be used to measure adhesive forces and has been used in other studies to measure the precise force of sub-cellular interactions such as protein-protein interactions.

When creating a platform for cell culture, how deeply a cell recognizes its surroundings becomes a pertinent question. One study created a standard “soft” polyacrylamide hydrogel akin to the stiffness found in brain tissue and varied the thickness of the gel to determine when cells could feel the “hidden” surface underneath which was a glass surface. The study found that the cells began to exhibit morphological differences at around 10-20 µm thickness gels. [119] Therefore, for all AFM measurements, the hydrogel platforms were not created in as thin films but at least 500 µm in height.

5.3.2. Radical polymerization to create a second-generation platform

Radical polymerization is an efficient way of making a uniform, homogeneous hydrogel network. Irgacure 2959 (I2959) is a well-known and established radical polymerizing agent that has been utilized in a variety of hydrogel-based studies to study stem cells or cancer. [13,15] Radical polymerization buffer (RPB) was formed by dissolving Irgacure 2959 into PBS for a final concentration of 0.5 wt%. MHyA was dissolved in RPB on the shaker for 1 hour at room temperature. The MHyA solution in RPB was mixed with thiol-modified PhyB and thiol-modified PIF6 and reacted, through click chemistry, for 24 hours at room temperature to enable binding of the proteins to the MHyA polymer.

Simultaneously, glass slides were functionalized with methacrylate groups. First, glass was exposed to oxygen plasma for 1 minute. A solution of 3-(Trimethoxysilyl) propyl methacrylate, acetic acid, and ethanol was mixed in a volumetric ratio of 2:3:5, respectively, and added to the oxygen-activated glass for 1 hour at room temperature. The glass slide was washed with DI water and dried with nitrogen gas.

Free strand hyaluronic polymers were created via sulfo-NHS/EDC chemistry. EDC and HyA polymers was dissolved in 0.1M MES (2-ethanesulfonic acid) buffer for a final EDC concentration of 50 mg/mL. Simultaneously, sulfo-NHS was dissolved in a second buffer (0.2M NaOH into PBS) at a concentration of 100 mg/mL. The EDC solution, sulfo-NHS solution, thiol-modified PhyB solution (2 mg/mL), thiol-modified PIF6 solution (2 mg/mL), were added at a ratio of 8:1:1:1. After 15 minutes at room temperature, the free strand was mixed with the MHyA in RPB at various ratios. The final hydrogel solution was plated onto the methacrylate-functionalized glass slides and exposed to 302 nm UV light for 10 minutes. The hydrogels were then allowed to swell in PBS for 24 hours before AFM measurements were taken.

5.4. Material properties of the hydrogel platform

5.4.1. Force of indentation influence on stiffness measurements

During the setup of the AFM measurements, the deflection trigger point is set uniformly throughout all measurements and is the distance which the cantilever will enter the sample before retracting. Based on the deflection trigger, the apparent stiffness of a

radical polymerized hydrogels differed per measurement (Figure 20). This could be for a couple reasons: there could be an actual stiffness gradient within the gel or there exists an “apparent” stiffness difference based on the deflection trigger point. Because of the adhesive properties of the Hystem-C™ hydrogels, the deflection trigger was set to 25 or 50 nm for all subsequent experiments. Otherwise, the cantilever would be unable to retract and overcome the adhesive force, limiting the ability of the AFM to take more than one measurement at a time. Additionally, for some very soft materials, the cantilever could only attain a maximum deflection of 25 or 50 nm when fully lowered. For future work, modulating the surface the hydrogel may prove necessary. A less adhesive surface would enable measurements with higher deflection points, which may be more accurate for measuring the hydrogel stiffness.

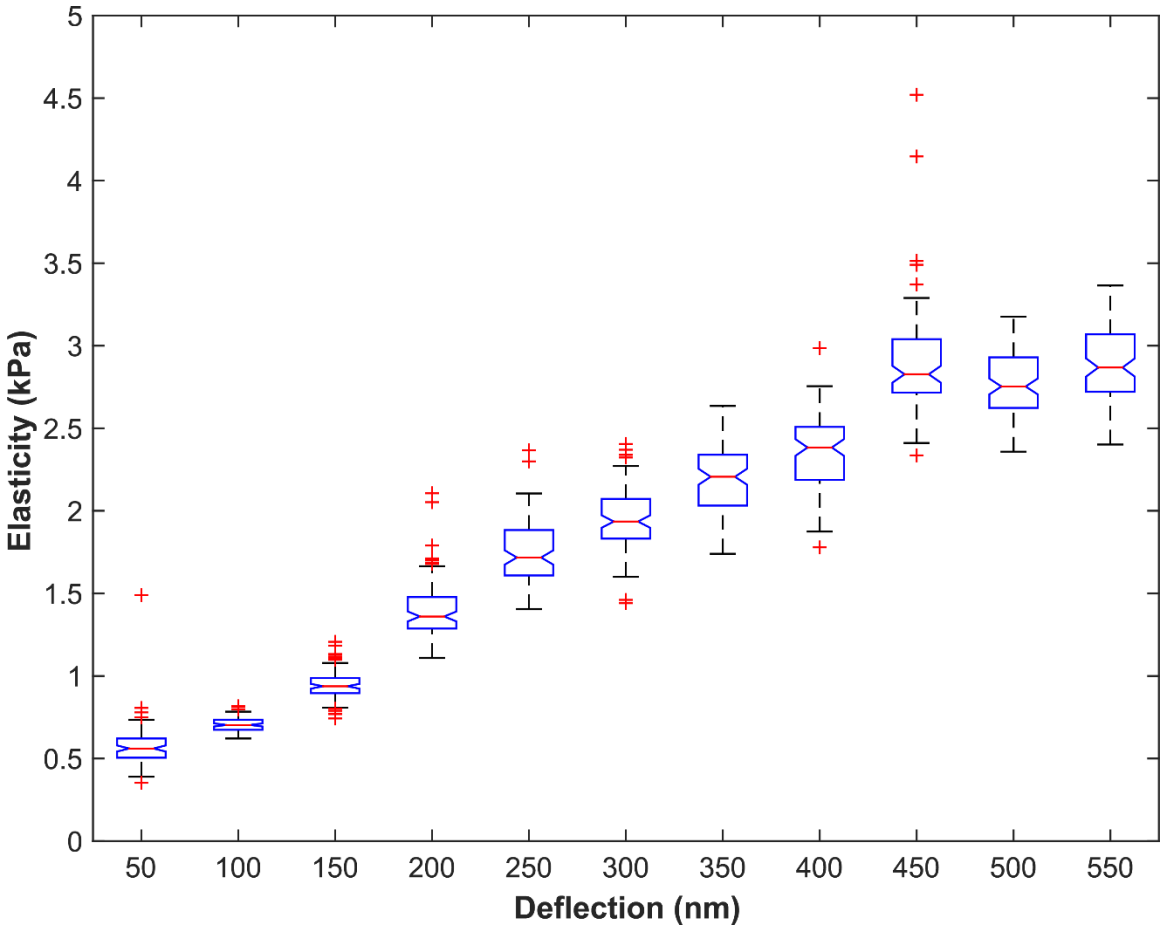

Figure 20. Deflection trigger influence on elasticity measurements.

All measurements were taken on the same 20 µm x 20 µm area on a 10 wt% MHyA (degrees of methacrylation of ~20%, 60 kDa in length) hydrogel that was crosslinked via a final solution of 0.5 wt% Irgacure 2959 in PBS with 302 nm UV light for 10 minutes. (n=100 per measurement)

5.4.2. Free strand incorporation into the hydrogel network proven necessary for stiffness changes

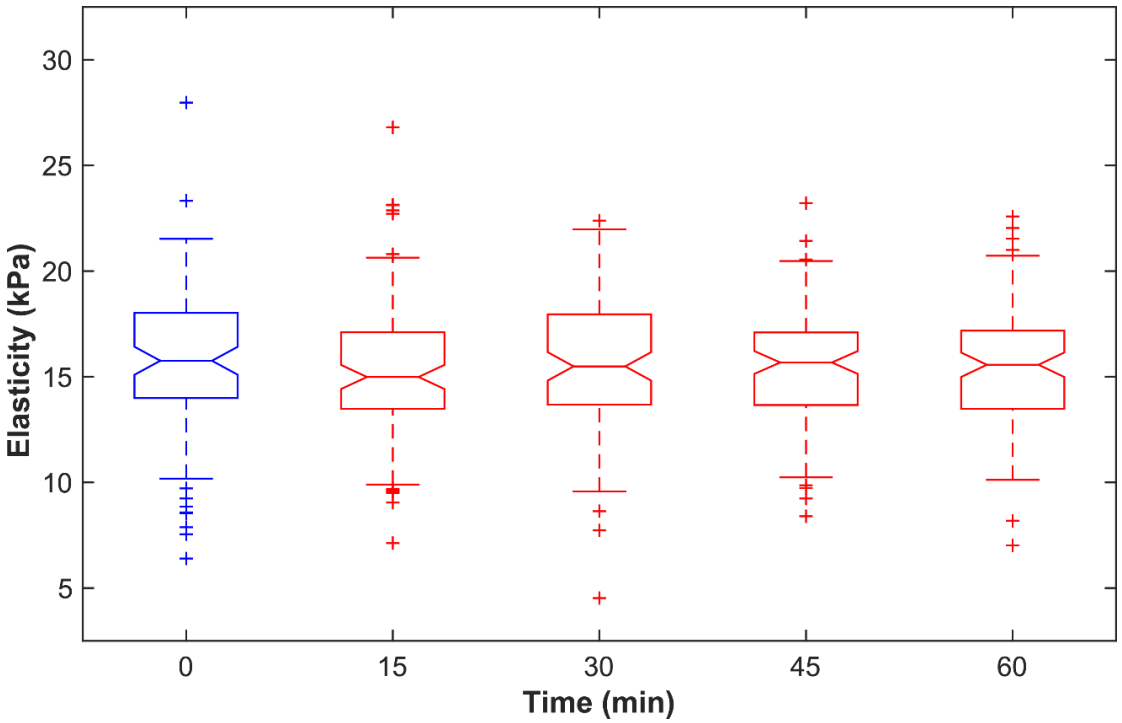

Figure 21. Hydrogel platform stiffness changes are insignificant without incorporation of the free strand.

Measurements were taken over a 10 µm x 10 µm area with a deflection trigger of 50 nm. Hydrogels were all created with 0.8 wt% Hystem™, 0.8 wt% Gelin-S™, 0.8 wt% Extralink from the Hystem-C™ kit (ESI BIO). PhyB and PIF6 were added to a final concentration of 20 µg/mL. Measurements were then taken as 650 nm light was continuously exposed to the hydrogel platform over an hour. (n=100 points per measurement). There was no statistically significant change in stiffness throughout the experiment.

During the course of this dissertation, it became apparent that the base network alone was unable to change stiffness based on light cues. One potential reason is that the network lacks the flexibility necessary to allow for additional crosslinks to form within itself. It is also possible that the hydrogel exhibited very slow kinetics for stiffness changes such that it took much longer than the course of an hour to exhibit any measurable differences. (Figure 21)

The free strand was incorporated to create the final semi-IPN hydrogel platform discussed in this dissertation because it would allow for more flexibility and opportunities for new crosslinks. In this system, the free strand would have more mobility to interact with the base network to create an increased crosslink density. Additionally, it was hypothesized that the strand would only need to diffuse across a limited distance, no more

than the average mesh size of the base hydrogel, to create stiffness changes. Subsequent experiments that include the free strand into the hydrogel platform were able to exhibit changes in stiffness. (Figures 22-26)

The semi-IPN hydrogel platform was able to stiffen and loosen based on the wavelength of light as measured with AFM during a time-exposure experiment. (Figure 22) However, the hydrogel platform did not seem capable of stiffening to the previous peak stiffness a second time. Some possible explanations for this phenomenon could include a deactivation period of PhyB after its conformational shift. Other potential

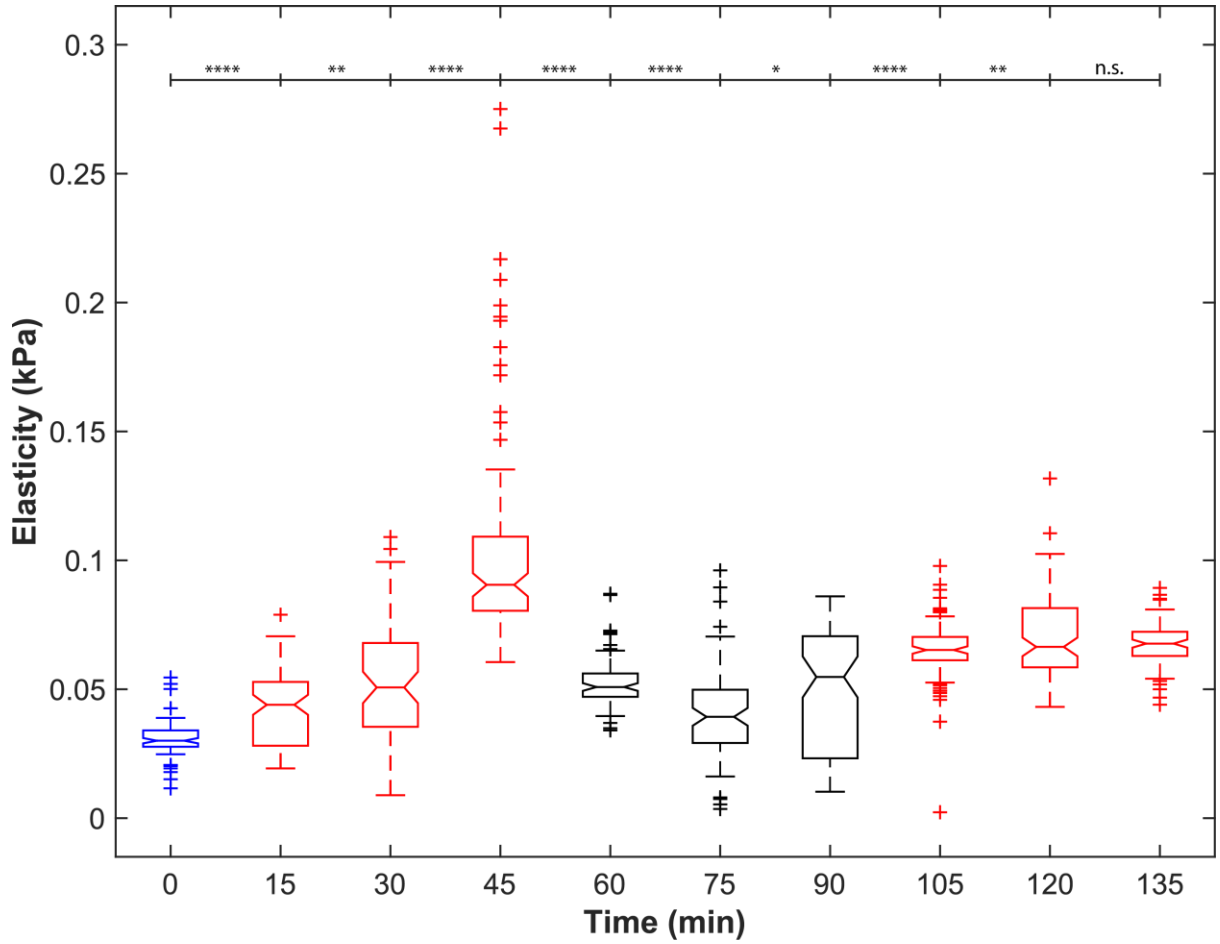

Figure 22. Hydrogel platform stiffness changes with incorporation of free strand.

Measurements were taken over a 10 µm x 10 µm area with a deflection trigger of 25 nm. Hydrogels were all created with 0.4 wt% Hystem™, 0.4 wt% Gelin-S™, 0.4 wt% Extralink from the Hystem-C™ kit (ESI BIO). PhyB and PIF6 were added to a final concentration of 20 µg/mL. The free strand was made of MHyA (40 kDa, degrees of methacrylation ~10%) and had a final concentration of 0.12 wt%. Light at either 650 nm or 750 nm light was exposed to the hydrogel platform alternating every 45 minutes. The red boxes depict the times when 650 nm light was exposed, and the black boxes are when 750 nm light was exposed. Significance is shown above the box plots. (n=100 points per measurements). *P<0.05, **P<0.01, ***P<0.001, ****P<0.0001

explanations could be that certain areas created highly strained crosslinks that could not reform when activated a second time. This was determined by looking at the stiffness of individual points over time. Some showed an ability to re-stiffen to a similar magnitude and some points which exhibited high stiffness changes were unable to stiffen again to the same magnitude. (Figure 23)

Future studies should investigate whether the activity of the PhyB and the kinetics of the Pr to Pfr conformational shift can be repeatedly recreated. Furthermore, changing the density of the base network and the degrees of methacrylation of the free strand may further elucidate the ability of the hydrogel platform to change stiffness repeatedly.

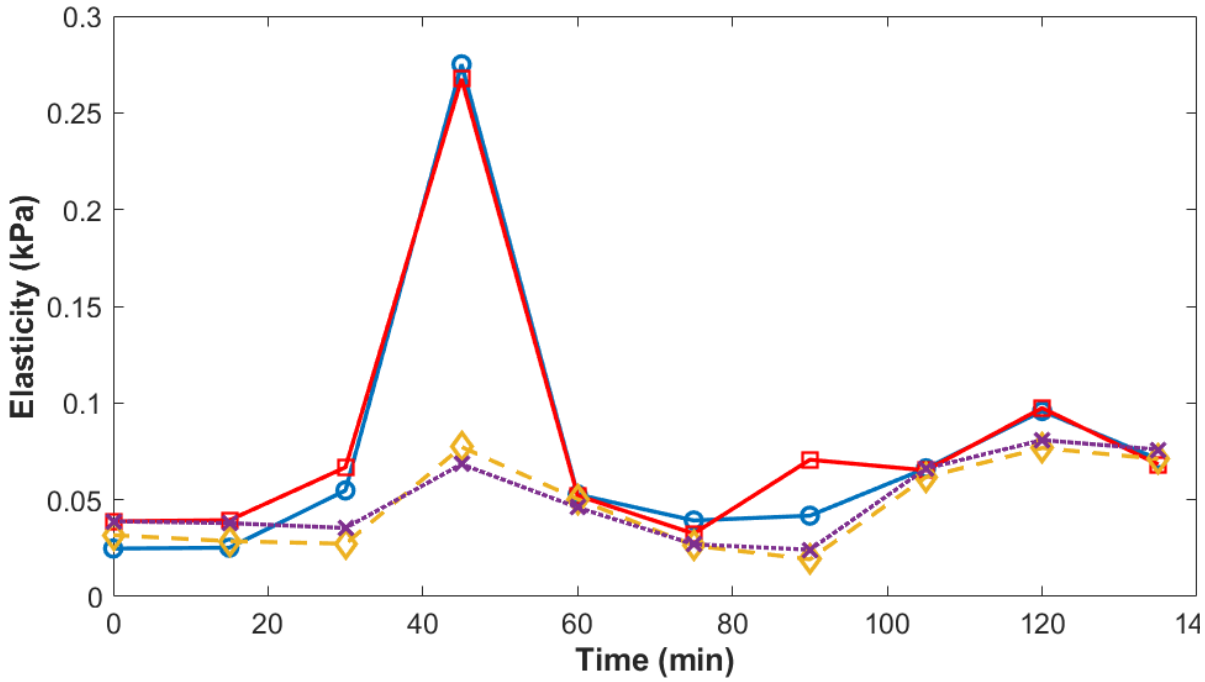

Figure 23. Stiffness changes at individual points from Figure 22.

5.4.3. Influence of light intensity on the hydrogel platform

For all experiments, a fluorescent mercury lamp was filtered via optical filters to create multiple wavelength sources. The filtered light could then be presented to the sample through a diffuse objective or directly. Predictably, the diffused light was less intense than the direct light source. The direct light was aimed through visual inspection via a microscope camera to the area where the cantilever hovered above.

Comparing the effects from diffuse and direct light sources on the hydrogel platform elucidated that the platform requires a minimum intensity of light to induce stiffness changes. (Figure 24) When the indirect light entered the gel, the gel decreased its stiffness. This could be because the gel, after being exposed to 750 nm light for 1 hour before the experiment, was still softening. As found in previous experiments (data not

shown), delays of up to 15 minutes in stiffness can occur even after switching the light source. This delay in response could be due to the viscoelastic nature of the hydrogel platform. Future steps should investigate this delay in stiffness changes and whether altering the composition of the hydrogel platform can shorten this delay. The direct light source was able to dramatically shift the stiffness of the hydrogel platform within 15 minutes. This suggests that there is a threshold power at which the PhyB proteins require to change conformation. Future studies should determine whether a gradient of light intensity will activate a gradient of percentage of activated PhyB proteins. If the percentage of activated PhyB can be controlled based on light intensity, the hydrogel platform could be patterned to have gradient stiffnesses.

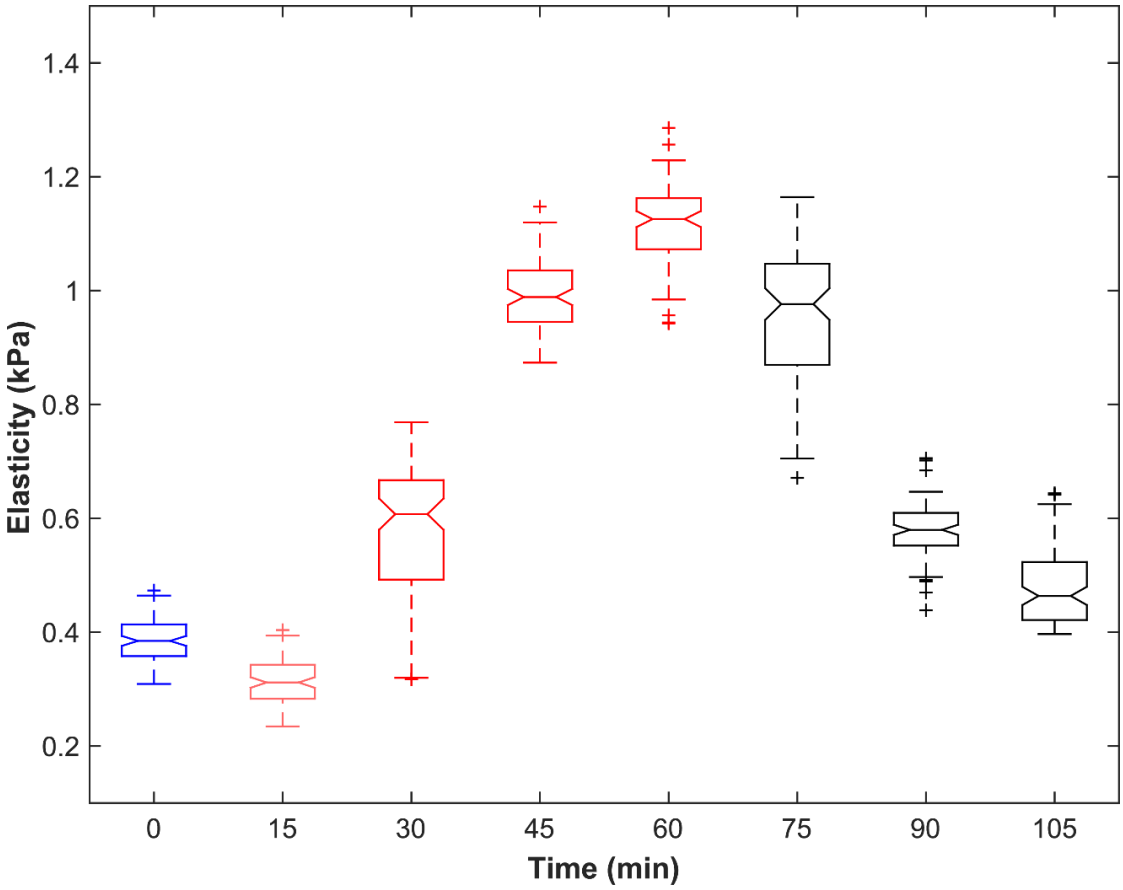

Figure 24. Hydrogel platform stiffness changes based on light intensity.

Measurements were taken over a 10 µm x 10 µm area with a deflection trigger of 25 nm. Hydrogels were all created with 0.4 wt% Hystem™, 0.4 wt% Gelin-S™, 0.4 wt% Extralink from the Hystem-C™ kit (ESI BIO). PhyB and PIF6 were added to a final concentration of 200 µg/mL. The free strand was made of MHyA (1 MDa, degrees of methacrylation ~1%) and had a final concentration of 0.01 wt%. For 15 minutes, diffuse 650 nm light was exposed before 45 minutes of direct 650 nm light. This was followed by 45 minutes of 750 nm light. The pink box represents when diffuse 650 nm light was exposed, the red boxes depict the times when direct 650 nm light was exposed and the black boxes when 750 nm light was exposed. All data sets were significant $p<0.0001$. (n=100 points per measurement)

5.4.4. Hydrogel platform stiffness retention without light cues

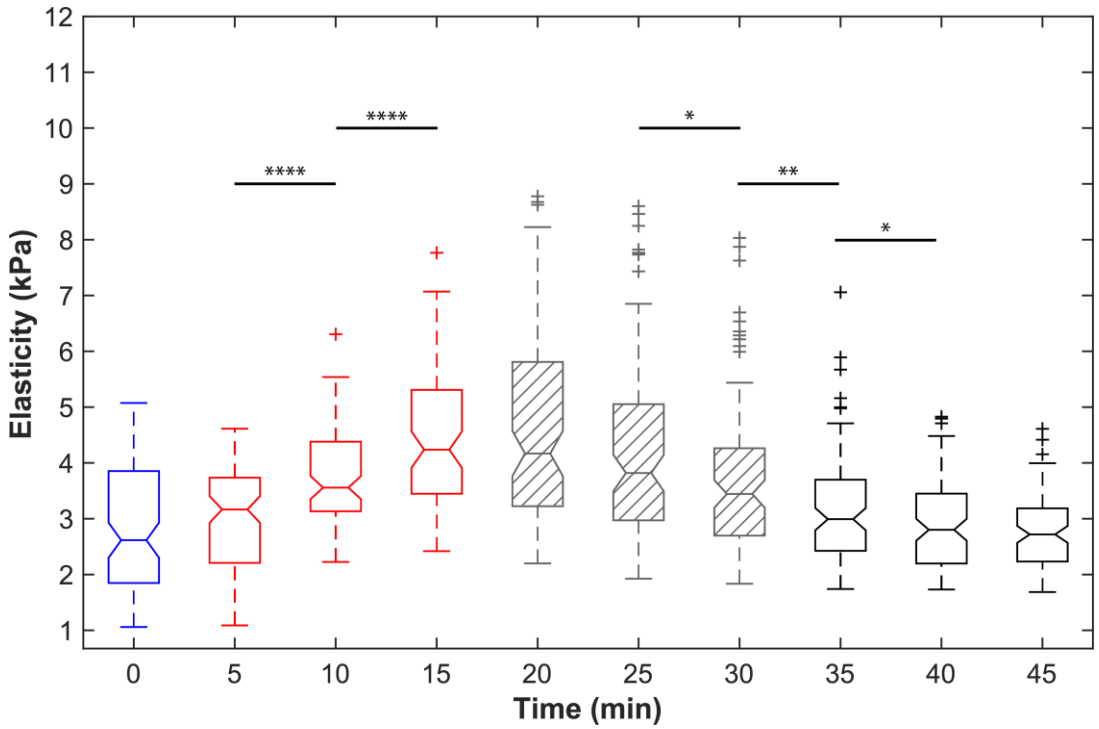

Figure 25. Hydrogel platform stiffness retention in the absence of light cues.

Measurements were taken over a 10 µm x 10 µm area with a deflection trigger of 50 nm. Hydrogels were all created with 0.4 wt% Hystem™, 0.4 wt% Gelin-S™, 0.8 wt% Extralink from the Hystem-C™ kit (ESI BIO). PhyB and PIF6 were added to a final concentration of 200 µg/mL. The free strand was MHyA (40 kDa, degrees of methacrylation ~10%) and had a final concentration of 0.4 wt%. Light at 650 nm was exposed to the hydrogel platform for 15 minutes before all light was turned off for an additional 15 minutes. Finally, 750 nm light was exposed for the final 15 minutes. The red boxes depict the times when 650 nm light was exposed, the grey shaded boxes depict the times when no light was exposed, and the black boxes when 750 nm light was exposed. Significance is shown above the box plots (n=100 points per measurement) *P<0.05, **P<0.01, ****P<0.0001

The ability for the platform to retain its stiffness without light cues would demonstrate the ability of PhyB to maintain its Pfr conformational state without continuous light stimulation. The hydrogel platform can maintain some stiffness without light cues but will decrease its stiffness more rapidly with the 750 nm light source. (Figure 25) Individual points within the hydrogel seem to vary in their abilities to retain stiffness changes. Some points were able to maintain some of their stiffness throughout the no-light period until the 750 nm light turns on. Others lose part or most of their stiffnesses immediately after the 650 nm light is turned off but will also soften further when the 750 nm light turns on. (Figure 26) It should be noted that the stiffness of this hydrogel platform was higher than other measurements because of the increased concentration of crosslinker (Extralink®) used on the base hydrogel.

Potential explanations for the immediate loss in stiffness could be due to PhyB inactivation or breaks in crosslinks due to mechanical strain. The diversity of relaxation of points also demonstrates that not all the PhyB deactivates immediately upon loss of light stimulation. The partial retention of the hydrogel platform to hold its stiffness indicates that potentially continual light cues are not necessary to maintain hydrogel stiffness. However, future work should investigate the retentive abilities of the hydrogel platform based on multiple considerations including free strand and protein concentration or the exposure time of light stimuli.

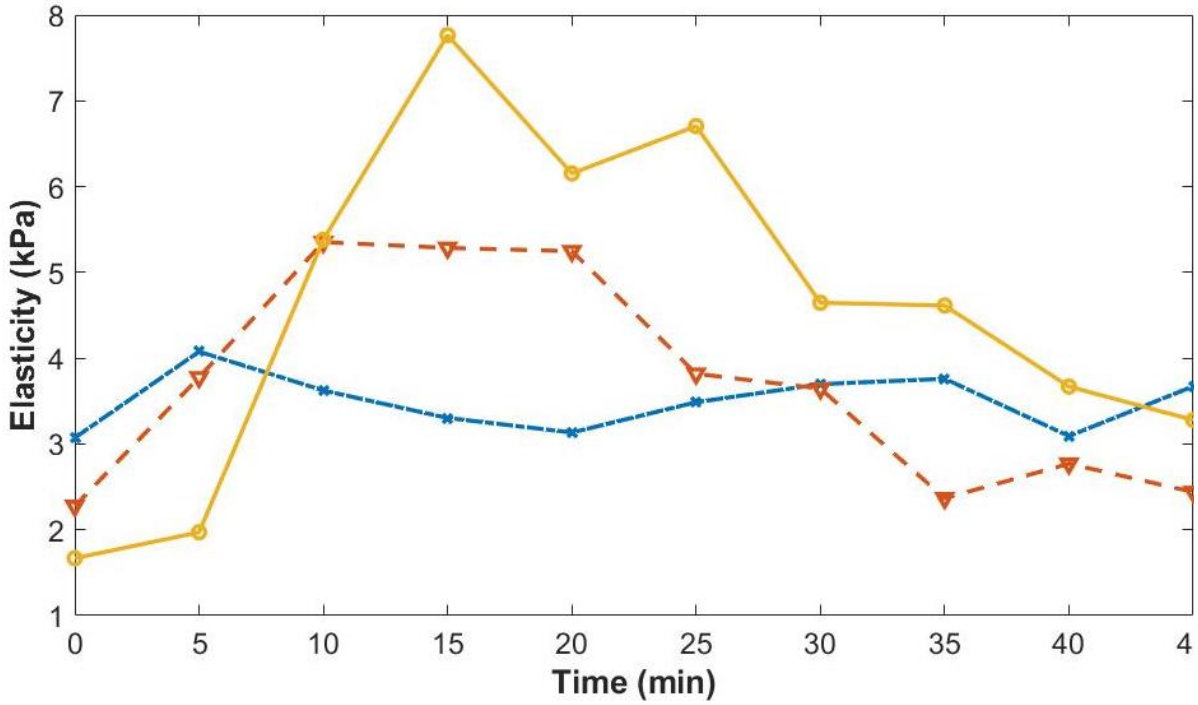

Figure 26. Stiffness changes at individual points from Figure 25.

5.4.5. Methacrylated hydrogel platform stiffness changes

While most of the experiments in this chapter have utilized hydrogel platforms made through click chemistry, the thiol-ene reaction for hydrogel gelation proved to create large ranges of stiffness throughout the measured area. In Figures 25, the range of stiffness of the hydrogel was over 2 kPa. Additionally, measurements at different areas of the same hydrogel platform could have up to a twofold difference in stiffness (data not shown). To create a hydrogel platform to study the effects of matrix rigidity on cellular processes, the variance of stiffness should be made as narrow as possible.

Because the Hystem-C™ platform required thiol-ene chemistry and combining viscous polymer solutions, it was hypothesized that the relatively quick reaction time of thirty minutes limited the ability for sufficient mixing, leading to the large stiffness variance within the same hydrogel platform. For a secondary hydrogel platform, radical chemistry

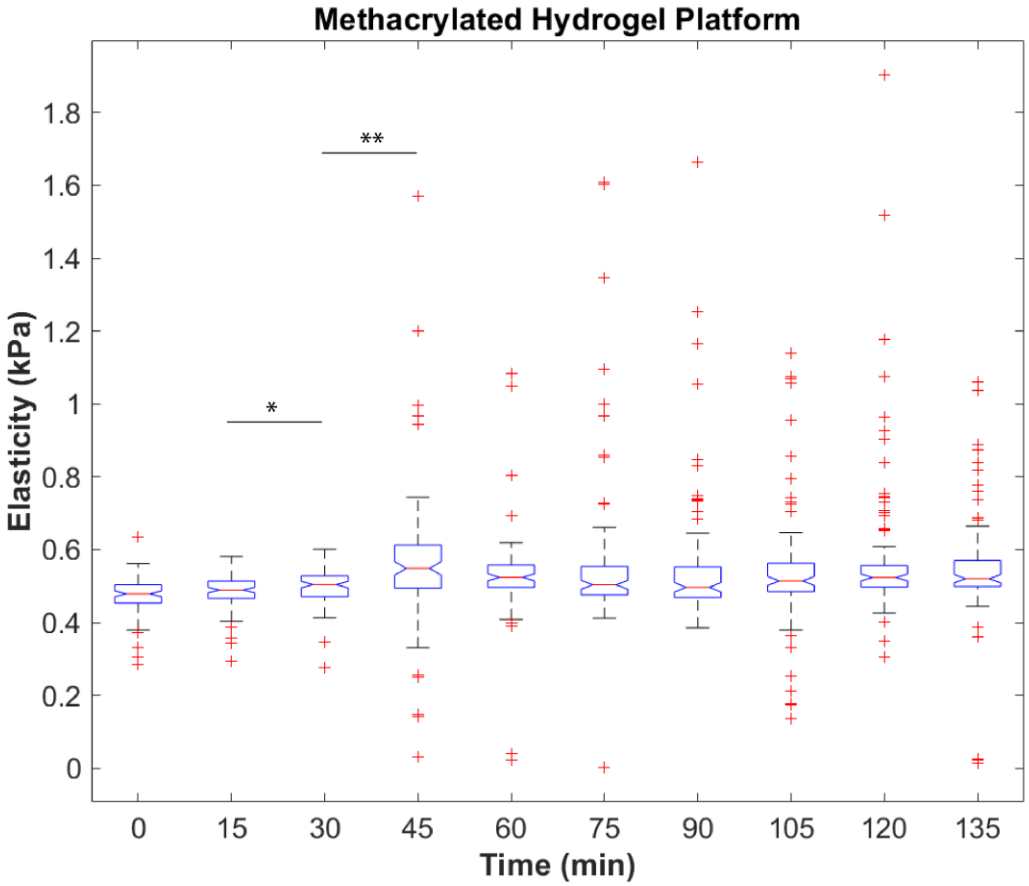

Figure 27. Methacrylate hyaluronic hydrogel platform.

Measurements were taken over a 50 µm x 50 µm area with a deflection trigger of 50 nm. Hydrogels were all created with MHyA (60 kDa, degrees of methacrylation ~20%) and had a final concentration of 8 wt%. The free strand was a sulfo-NHS/EDC functionalized polymer with a final concentration of 2 wt%. Light of 650 nm was exposed to the hydrogel platform for 135 minutes. (n=100 pts for each measurement) *P<0.05, **P<0.01

was used to create the base network and native HyA polymers reacted with sulfo-NHS/EDC to conjugate proteins served as the free polymer strand. Radical chemistry can be initiated by a UV light source and so these hydrogel solutions can be thoroughly mixed before gelation.

This secondary hydrogel platform had a much more consistent stiffness between multiple areas of measurement. However, time-exposure experiments revealed that the hydrogel was unable to form the dramatic stiffness changes seen in the first hydrogel platform. (Figure 27) Although some stiffness changes were seen around 30 to 45 minutes of exposure, the average difference in stiffness were limited to less than 10% of the original stiffness. It is possible that the hydrogel has a limited amount of flexibility or mobility due to the nature of radical polymerization chemistry. For future work, altering the degrees of methacrylation of the MHyA polymers or decreasing the photoinitiator

concentration may allow the second-generation hydrogel platform to see more dramatic stiffness changes.

5.5. Discussion

This chapter utilized atomic force microscopy (AFM) to determine the stiffness changes of the hydrogel platform discussed in this dissertation. While there are other methods of measuring substrate elasticity, such as rheometers, the AFM was able to provide spatial stiffness resolutions which allowed insight into the stiffening and softening process of the hydrogel platform. One obstacle of using the AFM was the adhesive nature of the hydrogel platform. Future work should include an investigation into coating mechanisms to limit the adhesive properties of the hydrogel platform to more accurately obtain stiffness measurements.

The hydrogel platform was able to demonstrate the ability of PhyB and PIF6 to serve as light-inducible crosslinkers and to induce material stiffness changes. In particular, the incorporation of a free polymer strand proved instrumental in inducing stiffness changes, potentially because the incorporation of the free strand increased the flexibility of the platform to form additional crosslinks. Although the hydrogel platform was able to demonstrate stiffness changes according to light cues, it was limited in its ability to achieve cyclical stiffening. It is possible that the hydrogel could have a “refractory” period in which the hydrogel cannot re-stiffen. Future work should determine the cause for this limitation, which could be due to an inability for PhyB to make multiple conformation changes or the viscoelastic nature of the hydrogel platform itself.

A more quantitative influence of light intensity on the stiffening would determine the stiffness-patterning potential of the platform. Additionally, the ability of the hydrogel platform to maintain its stiffness without light cues seems varied based on the location within the hydrogel platform. Identifying and quantifying both the influence of intensity and absence of light cues would be useful when considering stiffness patterning on the platform.

Other future work could include changing the chemistries of the base hydrogel and free strand. The hydrogels were made from the Hystem-C™ which utilized Michael-addition based crosslinks and suffered from incomplete gelation and stiffness variations within the platform. The viscosity of the polymer solution and the rate of the gelation could have led to incomplete mixing and created an uneven stiffness profile. This inconsistency in stiffness presents a problem for any downstream cell culturing applications that investigate the influence of matrix rigidity on cellular processes.

Finally, a secondary platform utilizing radical polymerization for the base hydrogel proved to have more consistent stiffnesses throughout the platform. Hydrogels that have implemented radical chemistries have also been successfully utilized to culture sensitive cell lines in previous studies. [120,121] However, the second-generation platform had a much more limited ability to change stiffness than the first platform. It is possible that the radical polymerization led to a less flexible structure that limited the ability for the platform to create secondary light-induced crosslinks. Future studies should determine the effects

of photoinitiator concentration and degrees of methacrylation on the hydrogel platform's ability to have stiffness changes.

While the hydrogel platform proved capable of softening and stiffening based on light cues, robustness of the platform for downstream studies requires further optimization. Variance in protein concentration, polymer length, and light exposure are just some of many factors that will influence the stiffening potential of the hydrogel platform. Upon future development, this hydrogel platform could provide promising insight into the influence of a diverse range of mechanical stimuli on complex cellular processes.

Chapter 6. Summary and Future Work

Cells are highly influenced by their mechanical environments and have a dynamic array of proteins that help translate external mechanical cues into internal signals. As such, the rigidity of the cell culturing substrate has shown to have a profound impact on cancer progression, metastasis, and stem cell differentiation. Many have turned to creating dynamic-stiffness hydrogel platforms to more precisely investigate a wide variety of physical conditions, including the effects of temporal stiffness. UV light-based methods for changing hydrogel elasticity are advantageous in that they are immediately able to modulate elasticity. However, they are limited in their ability to induce reversible stiffness changes. DNA- and protein-based methods could induce reversible stiffnesses but are limited in their abilities to have rapid changes due to mass transport limitations or require changes in pH or temperature which are unsuitable for cell culture.

Using optogenetic proteins as a dynamic hydrogel crosslinker could combine the advantages of immediacy from the UV-responsive hydrogels and of reversibility from the DNA-based hydrogels while maintaining physiological conditions. PhyB and PIF6 specifically were chosen since their association and dissociation are activated at distinct wavelengths of light. Additionally, these wavelengths are found on the red/far-red end of the light spectrum which is less toxic than light from the blue to near-UV range. To create plasmids expressing these proteins, golden gate cloning was implemented because it enabled highly parallelized creation of plasmid constructs. PhyB and PIF6 were conjugated to various fluorescent proteins, such as CFP and YFP, were expressed in *E. coli*, and were purified via a combination of Ni-NTA, ion exchange, and size exclusion columns. The exogenous activity of these proteins could not be confirmed with FRET due to a poor signal-to-noise ratio. However, TIRF microscopy was successfully utilized to visualize the recruitment of GFP-PIF6 to a PhyB-conjugated glass slide.

Of the various hydrogel polymers, hyaluronic acid was chosen because it is capable of a wide variety of protein-conjugating and crosslinking chemistries. Furthermore, HyA hydrogels are transparent, which would enable complete penetration of light cues. In the platform presented in this dissertation, thiol-ene chemistry, which falls under the classification of click chemistry, was implemented for both protein conjugation and crosslinking of the hydrogel polymers. HyA was modified to have methacrylate groups and the modification was confirmed via ^{1}H NMR spectrometry. Confocal microscopy was used to visualize the successful conjugation of fluorescently-labeled PhyB and PIF6 to the hydrogel platform. Additionally, hMSCs were cultured on HyA hydrogels for six days to confirm its compatibility for long term cell culture.

Finally, AFM determined the ability of the hydrogel platform to change stiffness based on a variety of light cues. The platform was only able to show significant stiffness changes upon incorporation of a free polymer strand into the base hydrogel network or the creation of a semi-IPN structure. It was hypothesized that the free strand enabled a quicker response time due to its increased mobility which allowed for additional crosslink formation opportunities. It was also determined that there is a minimum threshold light intensity that is required to induce stiffness changes. Furthermore, the hydrogel platform has some ability to retain stiffness changes without light cues but seems to be area

specific. This suggests that crosslinks that are created with high strain are unable to maintain their connection without light cues. When the hydrogel base crosslinking chemistry was changed to radical polymerization, the hydrogel was unable to change stiffness as dramatically, suggesting that radical polymerization may not enable as much motility as the click chemistry-based platform.

For future work, the platform would benefit from a complete understanding of the influence of the following variables: hydrogel polymer length, degrees of methacrylation of the free strand, and overall protein concentration and purity. Potentially, varying the material of both the free strand and the base hydrogel to other polymers such as PEG could enable more consistent stiffness changes. Additionally, it has been suggested in literature that other truncated versions of PhyB and use of cofactor PΦB could make a more optimal protein-protein interaction between PhyB and PIF6. Although it was not fully explored in this dissertation, there are many other crosslinking chemistries that exist for protein conjugation and crosslinking within hyaluronic acid hydrogels. Because the current hydrogel platform suffers from a non-homogeneous stiffness distribution, potentially due to the nature of its gelation, a more uniform gelation strategy, such as radical polymerization, should be investigated.

Upon optimization, a more robust hydrogel platform could then be utilized to understand the influence of matrix stiffness pulses on stem cell differentiation. Understanding the “threshold” stimulation necessary to commit hMSCs to different lineages could help elucidate the nuances of mechanical-directed differentiation. Furthermore, the platform could be optimized to have patterning or gradient stiffnesses by varying light intensity and duration, which could be useful for observations of cell migration and cancer metastasis. Finally, this platform could also be re-engineered to enable 3D cell cultures which could even more closely mimic *in vivo* conditions for *in vitro* experiments.

Chapter 7. References

1. Stutchbury, B., Atherton, P., Tsang, R., Wang, D. Y. & Ballestrem, C. Distinct focal adhesion protein modules control different aspects of mechanotransduction. J. Cell Sci. 130, 1612–1624 (2017).
2. Discher, D. E., Janmey, P. & Wang, Y. L. Tissue cells feel and respond to the stiffness of their substrate. *Science.* 2005 Nov; 310(5751):1139-43, doi:10.1126/science.1116995
3. Ladoux, B. & Mege, Rene-Marc. Mechanobiology of collective cell behaviours. *Nature Review Molecular Cell Biology*. 2017 Dec; 18(12):743-757. doi: 10.1038/nrm.2017.98
4. Totaro, A., Panciera, T., & Piccolo, S. YAP/TAZ upstream signals and downstream responses. *Nature Cell Biology*. 2018 Aug; 20:888-899. doi: 10.1038/s41556-018-0142-z
5. Panciera, T., Azzolin, L., Cordenonsi, M, & Piccolo, S. Mechanobiology of YAP and TAZ in physiology and disease. *Nature Review Molecular Cell Biology*. 2017 Dec; 18(12):758-770. doi: 10.1038/nrm.2017.87
6. Uhler, Caroline & Shivashankar, G. V. Regulation of genome organization and gene expression by nuclear mechanotransduction. *Nature Review Molecular Cell Biology*. 2017 Dec; 18:717-727. doi: 10.1038/nrm.2017.101.
7. Nagelkerke, A., Bussink, J., Rowan, A. E. & Span, P. N. The mechanical microenvironment in cancer: How physics affects tumours. *Seminars in Cancer Biology*. 2015 Dec; 35:62-70. doi:10.1016/j.semcancer.2015.09.001
8. Ruppender, N. S., Merkel A.R., Martin, T.J., Mundy G.R., Sterling J.A. & Guelcher S.A. Matrix rigidity induces osteolytic gene expression of metastatic breast cancer cells. *PloS One.* 2010 Nov; 5(11): e15451, doi:10.1371/journal.pone.0015451
9. Charras, G. & Sahai, E. Physical influences of the extracellular environment on cell migration. *Nature Reviews Molecular Cell Biology*. 2014 Oct; 15, 813-24, doi:10.1038/nrm3897
10. Chaudhuri, O., Koshy, S. T., Branco da Cunha, C., Shin, J., Verbeke, C. S., Allison, K. H., & Mooney, D. J. Extracellular matrix stiffness and composition jointly regulate the induction of malignant phenotype in mammary epithelium. *Nature Materials.* 2014 Oct; 13:970-978. doi: 10.1038/nmat4009.
11. Engler, A. J., Sen, S., Sweeney, H. L. & Discher, D. E. Matrix elasticity directs stem cell lineage specification. *Cell.* 2006 Aug; 126, 677-689, doi:10.1016/j.cell.2006.06.044
12. Saha, K., Keung, A. J., Irwin, E. F., Li, Y., Little, L., Schaffer, D. V., & Healy, K. E. Substrate modulus directs neural stem cell behavior. *Biophysical Journal*. 2008 Nov; 95(9): 4426-38. doi:10.1529/biophysj.108.132217. Epub 2008 Jul 25.
13. Rape, A. D., Zibinsky, M., Murthy, N. & Kumar, S. A synthetic hydrogel for the high-throughput study of cell-ECM interactions. *Nature Communications*. 2015 May; 6, 8129, doi:10.1038/ncomms9129

14. Iwashita, M., Kataoka N., Toida K., & Kosodo, Y. Systematic profiling of spatiotemporal tissue and cellular stiffness in the developing brain. *Development*. 2014 Oct; 141(19):3793-8. doi: 10.1242/dev.109637.
15. Yang, C., Tibbit, M.W., Basta, L., and Anseth, K. Mechanical memory and dosing influence stem cell fate. *Nature Materials*. 2014 Jun; 13(6); 645-52. doi: 10.1038/nmat3889
16. Elkin, B. S., Azeloglu, E. U., Costa, K. D., & Morrison, B. Mechanical heterogeneity of the rat hippocampus measured by atomic force indentation. *Journal of Neurotrauma*. 2007 May; 24(5):812-22. doi:10.1089/neu.2006.0169
17. Tao, N. J., Lindsay, S. M., & Lees, S. Measuring the microelastic properties of biological material. *Biophysical Journal*. 1992 Oct; 63(4):1165-9. doi:10.1016/S0006-3495(92)81692-2
18. Vining, K. H. & Mooney, D. J. Mechanical forces direct stem cell behaviour in development and regeneration. *Nature Review Molecular Cell Biology*. 2017 Dec; 18(12): 728-742. doi:10.1038/nrm.2017.108.
19. Geckil, H., Xu, F., Zhang, X., Moon, S., & Demirci, U. Engineering hydrogels as extracellular matrix mimics. *Nanomedicine (Lond)*. 2010 Apr; 5(3):469-84. doi:10.2217/nnm.10.12
20. Denisin, A.K., & Pruitt, B. L. Tuning the range of polyacrylamide gel stiffness for mechanobiology applications. *ACS Applied Material Interfaces*. 2016 Jan; 8(34):21893-902. doi: 10.1021/acsami.5b09344
21. Scheideler, O. J., Sohn, L. L. & Schaffer, D. V. Emerging Engineering Strategies for Studying the Stem Cell Niche. *Biology in Stem Cell Niche*. 2015; 57-106 ac(Springer International Publishin). doi: https://doi.org/10.1007/978-3-319-21702-4_3
22. Lee, K. Y. & Mooney, D. J. Hydrogels for tissue engineering. *Chemical Reviews.* 2001 Jul; 101(7): 1869-1879
23. Mosiewicz, K. A., Kolb, L., van der Vlies, A. J., and Lutolf, M. P. Microscale patterning of hydrogel stiffness through light-triggered uncaging of thiols. *Biomaterial Science.* 2014 Jul; 2:1640-51
24. Guvendiren, M. & Budrick, J. A. Stiffening hydrogels to probe short- and long-term cellular responses to dynamic mechanics. *Nature Communications*. 2012 Apr; 3, 792. doi:10.1038/ncomms1792
25. Kloxin, A. M., Kloxin, C. J., Bowman, C. N. & Anseth, K. S. Mechanical properties of cellularly responsive hydrogels and their experimental determination. *Advanced materials.* 2010 Aug; 22(31):3484-94, doi:10.1002/adma.200904179
26. Kloxin, A. M., Tibbitt, M. W. & Anseth, K. S. Synthesis of photodegradable hydrogels as dynamically tunable cell culture platforms. *Nature protocols*. 2010 Dec; 5(12), 1867-87, doi:10.1038/nprot.2010.139
27. Rammensee, S., Kang, M. S., Georgiou, K., Kumar, S., & Schaffer, D. V. Dynamics of mechanosensitive neural stem cell differentiation. *Stem Cells* 2017 Feb; 35(2): 497-506 doi:10.1002/stem.2489
28. Miyata, T., Asami, N., & Uragami, T. Preparation of an antigen-sensitive hydrogel using antigen-antibody bindings. *Macromolecules*. 1999 Jan; 32: 2082-84

29. Miyata, T., Asami, N., & Uragami, T. A reversibly antigen-responsive hydrogel. *Nature*. 1999 Jun; 399:766-9
30. Lu, Z., Kopeckova, P., & Kopecek, J. Antigen responsive hydrogel based on polymerizable antibody Fab' fragment. *Macromolecule Biosciences*. 2003 Jun; 3:296-300. doi:10.1002/mabi.200390039
31. Rombouts, W. H., de Kort, D. W., Pham, T. T. H., van Mierlo, C. P. M., Werten, M. W. T., de Wolf, F. A., & van der Gucht, J. Reversible temperature-switching of hydrogel stiffness of coassembled, silk-collagen-like hydrogels. *Biomacromolecules.* 2015 Jul; 16(8): 2506-13. doi: 10.1021/acs.biomac.5b00766
32. Wang, C., Stewart, R. J., & Kopecek, J. Hybrid hydrogels assembled from synthetic polymers and coiled-coil protein domains. *Nature*. 1999 Feb; 397(6718):417-20.
33. King, W. J., Toepke, M. W., and Murphy, W. L. A general route for the synthesis of a functional, protein-based hydrogel microspheres using tailored protein charge. *Chemical Communications (Cambridge)*. 2011 Jan; 47(1): 526-528. doi: 10.1039/c0cc02716b.
34. Keung, A. J., Kumar, S., & Schaffer, D. V. Presentation counts: microenvironmental regulation of stem cells by biophysical and material cues. *Annual Review of Cell and Developmental Biology*. 2010 Jun; 26:533-56. doi:10.1146/annurev-cellbio-100109-104042
35. Lv, H., Li, L., Sun, M., Zhang, Y., Chen, L., Rong, Y., & Li, Y. Mechanism of regulation of stem cell differentiation by matrix stiffness. *Stem Cell Research & Therapy*. 2015 May; 6(1):103. doi:10.1186/s13287-015-0083-4
36. Li, D., Zhou, J., Chowdhury, F., Cheng, J., Wang, N. & Wang, F. Role of mechanical factors in fate decisions of stem cells. *Regenerative Medicine*. 2011 Mar; 6(2), 229-40, doi:10.2217/rme.11.2
37. Sun, L., Lee, J., & Fine, H. A. Neuronally expressed stem cell factor induces neural stem cell migration to areas of brain injury. *Journal of Clinical Investigation*. 2004 May; 113(9):1364-1374.
38. Zhao, W., Li, X., Liu, X., Zhang, N., & Wen, X. Effects of substrate stiffness on adipogenic and osteogenic differentiation of human mesenchymal stem cells. *Material Science and Engineering: C*. 2014 Jul; 40: 316-23
39. Trappmann, B., Gautrot, J. E., Connelly, J. T., Strange, D. G. T., Li, Y., Oyen, Michelle L., Stuart, M. A. C., Boehm, H., Li, B., Vogel, V., Spatz, J. P., Watt, F. M., & Huck, W. T. S. Extracellular-matrix tethering regulates stem cell fate. *Nature Materials*. 2012 Jul; 11:642-9. doi:10.1038/NMAT3339
40. Wen, J. H., Vincent, L. G., Fuhrmann, A., Choi. Y. S., Hribar, K. C., Taylor-Weiner, H., Chen, S., & Engler, A. J. Interplay of matrix stiffness and protein tethering in stem cell differentiation. *Nature Materials*. 2014 Oct; 13:979-87. doi:10.1038/NMAT4051
41. Reilly, G. C., & Engler, A. J. Intrinsic extracellular matrix properties regulate stem cell differentiation. *Journal of Biomechanics*. 2010 Jan; 43(1):55-62. doi:10.1016/j.jbiomech.2009.09.009

42. Keung, A. J., Healy, K. E., Kumar, S., & Schaffer, D. V. Biophysics and dynamics of natural and engineered stem cell microenvironments. *Wires Systems Biology and Medicine*. 2010 Jan; 2(1):49-64. doi:10.1002/wsbm.46
43. Pedrón S., Peinado, C., Bosch, P., & Anseth K. Synthesis and characterization of degradable bioconjugated hydrogels with hyperbranched multifunctional cross-linkers. *Acta Biomater.* 2010 Nov; (6)11:4189-4198. doi:10.1016/j.actbio.2010.06.005
44. Deforest, C. A., Sims, E. A. & Anseth, K. S. Peptide-Functionalized Click Hydrogels with Independently Tunable Mechanics and Chemical Functionality for 3D Cell Culture. Chemistry of materials : a publication of the American Chemical Society 22, 4783-4790, doi:10.1021/cm101391y (2010).
45. Kloxin, A. M., Kasko, A. M., Salinas, C. N. & Anseth, K. S. Photodegradable hydrogels for dynamic tuning of physical and chemical properties. Science 324, 59-63, doi:10.1126/science.1169494 (2009).
46. Musoke-Zawedde, P. & Shoichet, M. S. Anisotropic three-dimensional peptide channels guide neurite outgrowth within a biodegradable hydrogel matrix. Biomed. Mater. 1, 162-169 (2006).
47. Marklein, R. A. & Burdick, J. A. Spatially controlled hydrogel mechanics to modulate stem cell interactions. Soft Matter 6, 136-143 (2010).
48. Kloxin, A. M., Tibbitt, M. W., Kasko, A. M., Fairbairn, J. A. & Anseth, K. S. Tunable hydrogels for external manipulation of cellular microenvironments through controlled photodegradation. Advanced materials 22, 61-66, doi:10.1002/adma.200900917 (2010).
49. Petka, W. A., Harden, J. L., McGrath, K. P., Wirtz, D., & Tirrell, D. A. Reversible hydrogels from self-assembling artificial protein. *Science*. 1998 Jul; 281:389-92. doi:10.1126/science.281.5375.389
50. Stile, R. A., & Healy, K. E. Thermo-responsive peptide-modified hydrogel for tissue regeneration. *Biomacromolecules*. 2001 Feb; 2(1):185-94
51. Jeong, B., Kim, S. W., & Bae, Y. H. Thermosensitive sol-gel reversible hydrogels. *Advanced Drug Delivery Reviews*. 2002 Jan; 54(1):37-51
52. Choi, M., Choi, J. W., Kim, S., Nizamoglu, S., Hahn, S. K., & Yun, S. H. Light-guiding hydrogels for cell-based sensing and optogenetic synthesis *in vivo*. *Nat Photonics*. 2013 Oct; 7:987-94. doi:10.1038/nphoton.2013.278
53. Pathak, G. P., Vrana, J. D., & Tucker, C. L. Optogenetic control of cell function using engineered photoreceptors. *Biological Cell*. 2013 Feb; 105(2):59-72. doi:10.111/boc.201200056
54. Zhang, K. & Cui, B. Optogenetic control of intracellular signaling pathways. *Trends in Biotechnology*. 2015 Feb; 33(2):92-100
55. Li, X., Wang, Q., Yu, X., Liu, H., Yang, H., Zhao, C., Liu, X., Tan, C., Klejnot, J., Zhong, D., & Lin, C. Arabidopsis cryptochrome 2 (CRY2) functions by the photoactivation mechanism distinct from the tryptophan (trp) triad-dependent photoreduction. *PNAS*. 2011 Dec; 108(51): 20844-20849. doi:10.1073/pnas.1114579108
56. Cashmore, A. R. Cryptochromes: enabling plants and animals to determine circadian time. *Cell*. 2003 Sept; 114(5):537-43

57. Ozgur, S. & Sancar, A. Purification and properties of human blue-light photoreceptor cryptochrome 2. *Biochemistry*. 2003 Jan; 42:2926-32. doi:10.1021/bi026963n
58. Habuchi, S., Ando, R., Dedecker, P., Verheijen, W., Mizuno, H., Miyawaki, A., & Hofkens, J. Reversible single-molecule photoswitching in the GFP-like fluorescent protein Dronpa. *PNAS*. 2005 Jul; 102(27):9511-16. doi:10.1073/pnas.0500489102
59. Ni, M., Tepperman, J. M., & Quail, P. H. Binding of phytochrome B to its nuclear signaling partner PIF3 is reversibly induced by light. *Nature*. 1999 Aug; 400:781-4
60. Burgie, E. S., Bussell, A. N., Walker, J. M., Dubiel, K. & Vierstra, R. D. Crystal structure of the photosensing module from a red/far-red light-absorbing plant phytochrome. *PNAS*. 2014 Jul; 111(28): 10179-84. doi:10.1073/pnas.1403096111
61. Castillon, A., Shen, H., & Huq, E. Phytochrome Interacting Factors: central players in phytochrome-mediated light signaling networks. *TRENDS in Plant Science*. 2007 ; 12(11):1360-85. doi:10.1016/j.tplants.2007.10.001
62. Zhang, J., Stankey, R. J., & Vierstra, R. D. Structure-guided engineering of plant phytochrome B with altered photochemistry and light signaling. *Plant Physiology*. 2013 Mar; 161:1445-1457. doi:10.1104/pp.112.208892
63. Levskaya, A., Weiner, O. D., Lim, W. A. & Voigt, C. A. Spatiotemporal control of cell signalling using a light-switchable protein interaction. *Nature.* 2009 Oct; 461(7266), 997-1001, doi:10.1038/nature08446
64. Engler, C., Kandzia, R., & Marillonnet, S. A one pot, one step, precision cloning method with high throughput capability. *PLoS One.* 2008 Nov; 3(11): e3647. doi: 10.1371/journal.pone.0003647
65. Lee, M. E., DeLoache, W. C., Cervantes, B. & Dueber, J. E. A Highly Characterized Yeast Toolkit for Modular, Multipart Assembly. *ACS synthetic biology*. 2015 Sept; 4(9), 975-986, doi:10.1021/sb500366v
66. Engler, C., Gruetzner, R., Kandzia, R., & Marillonnet, S. Golden Gate Shuffling: a one-pot DNA shuffling method based on type IIs restriction enzymes. *PLoS ONE.* 2009 May; 4(5):e5553. doi:10.1371/journal.pone.0005553
67. Gambetta, G. A. & Lagarias, J. C. Genetic engineering of phytochrome biosynthesis in bacteria. *Molecular and Cellular Biology*. 2001 Sept; *PNAS*. 98(19):10566-71. doi:10.1073/pnas.191375198
68. Mukougawa, K., Kanamoto, H., Kobayashi, T., Yokota, A., & Kohchi, T. Metabolic engineering to produce phytochromes with phytochromobilin, phycocyanobilin, or phycoerythrobilin chromophore in *Escherichia coli*. *FEBS Letters*. 2006 Jan; 580:1333-8. doi:10.1016/j.febslet.2006.01.051
69. Schmidl, S. R., Sheth, R. U., Wu, A., & Tabor, J. J. Refactoring and optimization of light-switchable *Escherichia coli* two component systems. *ACS Synthetic Photobiology*. 2014 Sept; 3:820-31. doi:10.1021/sb500273n
70. Burgie, E. S., Bussell, A. N., Lye, S., Wang, T., Hu, W., McLoughlin, K. E., Weber, E. L., Li, H., & Vierstra, R. D. Photosensing and thermosensing by phytochrome B require both proximal and distal allosteric features within the dimeric

photoreceptor. *Scientific Reports*. 2017 Jun; 7, 13648. doi: 10.1038/s41598-017-14037-0
71. Kogan, G., Soltes, L., Stern, R., & Gemeiner, P. Hyaluronic acid: a natural biopolymer with a broad range of biomedical and industrial applications. *Biotechnology Letters* (2007) 29:17-25. doi: 10.1007/s10529-006-9219-z
72. Burdick, J.A., & Prestwich, G. D. Hyaluronic acid hydrogel for biomedical applications. *Advanced Materials* (2011) 23,H41-H56. doi:10.1002/adma.201003963
73. Collins, M. N., & Birkenshaw, C. Hyaluronic acid based scaffolds for tissue engineering – a review. *Carbohydrate Polymers* (2013). 92:1262-1279. doi:10.1016/j.carbpol.2012.10.028
74. Gerecht, S., Burdick, J.A., Ferreria, L.S., Townsend, S.A., Langer, R., & Vunjak-Novakovic, G. Hyaluronic acid hydrogel for controlled self-renewal and differentiation of human embryonic stem cells. *PNAS* (2007) 104(27):11298-11303. doi: 10.1073/pnas.0703723104
75. Lam, J., Truong, N. F., & Segura, T. Design of cell-matrix interactions in hyaluronic acid hydrogel scaffolds. *Acta Biomaterialia* (2014) 10:1571-1580. doi: 10.1016/.actabio.2013.07.025
76. Kurisawa, M., Chung, J. E., Yang, Y. Y., Gao, S. J., & Uyama, H. Injectable biodegradable hydrogels composed of hyaluronic acid-tyramine conjugates for drug delivery and tissue engineering. *Chemical Communications* (2005) 34: 4312-4314. doi: 10.1039/b506989k
77. Mero, A., Pasqualin, M., Campisi, M., Renier, D., & Pasut, G. Conjugation of hyaluronan to proteins. *Carbohydrate Polymers* (2013) 92:2163-2170. doi: 10.1016/j.carbpol.2012.11.090
78. Bulpitt, P. & Aeschlimann, D. New strategy for chemical modifications of hyaluronic acid: preparation of functionalized derivatives and their use in the formation of novel biocompatible hydrogels. *Journal of Biomedical Materials Research* (1999) 47(2): 152-69. doi: 10.1002/(SICI)1097-4636(199911)47:2<152::AID-JBM5>3.0.CO;2-I
79. Prestwich, G. D., Marecak, D. M., Marecak, J. F., Vercruysse, K. P., & Ziebell, M. R. Controlled chemical modification of hyaluronic acid: synthesis applications, and biodegradation of hydrazide derivatives. *Journal of Controlled Release* (1998) 53: 93-103. doi:10.1016/S0168-3659(97)00242-3
80. Wall, S. T., Saha, K., Ashton, R. S., Kam, K. R., Schaffer, D. V., & Healy, K. H. Multivalency of sonic hedgehog conjugated to linear polymer chains modulates protein potency. *Bioconjugate Chemistry* (2008) 19:806-812. doi: 10.1021/bc700265k
81. Collins, M. N. & Birkinshaw, C. Comparison of the effectiveness of four different crosslinking agents with hyaluronic acid hydrogel films for tissue-culture applications. *Journal of Applied Polymer Science* (2007) 104:3183-3191. doi: 10.1002/app.25993
82. Luo, Y., Kirker, K. R., & Prestwich, G. D. Crosslinked hyaluronic acid hydrogel films: new biomaterials for drug delivery. *Journal of Controlled Release* (2000) 69(1):169-184. doi:10.1016/S0168-3659(00)00300-X

83. Tuo, W. S., Lim, T. C., Kurisawa, M., & Spector, M. Modulation of mesenchymal stem cell chondrogenesis in a tunable hyaluronic acid hydrogel microenvironment. *Biomaterials* (2012) 33:3835-3845. doi: 10.1016/j.biomaterials.2012.01.065
84. Tan, H., Ramirez, C. M., Miljkovic, N., Li, H., Rubin, Rubin, J. P., & Marra, K. G. Thermosensitive injectable hyaluronic acid hydrogel for adipose tissue engineering. *Biomaterials* (2009) 30:6844-6853. doi: 10.1016/j.biomaterials.2009.08.058
85. Segura, T., Andrew, B. C., Chung, P. H., Webber, R. E., Shull, K. R., & Shea, L. D. Crosslinked hyaluronic acid hydrogels: a strategy to functionalize and pattern. *Biomaterials* (2005) 26:359-371. doi: 10.1016/j.biomaterials.2004.02.067
86. Yoo, H. S., Lee, E. A., Yoon, J. J., & Park, T. G. Hyaluronic acid modified biodegradable scaffolds for cartilage tissue engineering. *Biomaterials* (2005) 26:1925-1933. doi: 10.1016/j.biomaterials.2004.06.021
87. Oudshoorn, M. H. M., Rissman, R., Bouwstra, J. A., & Hennik, W. E. Synthesis of methacrylated hyaluronic acid with a tailored degree of substitution. *Polymer* (2007) 48:1915-1920. doi:10.1016/j.polymer.2007.01.068
88. Ananthanarayannan, B., Kim, Y., & Kumar, S. Elucidating the mechanobiology of malignant brain tumors using a brain matrix-mimetic hyaluronic acid hydrogel platform. *Biomaterials* (2011) 32:7913-7923. doi: 10.1016/j.biomaterials.2011.07.005
89. Snyder, T. N., Madhavan, K., Miranda, I., Dregalla, R. C., & Park, D. A fibrin/hyaluronic acid hydrogel for the delivery of mesenchymal stem cells and potential for articular cartilage repair. *Journal of Biomedical Engineering* (2014) 8:10. doi: 10.1186/1754-1611-8-10
90. Burdick, J. A., Chung, C., Jia, X., Randolph, M. A., & Langer, R. Controlled degradation and mechanical behavior of photopolymerized hyaluronic acid networks. *Biomacromolecules* (2005) 6: 386-391. doi: 10.1021/bm049508a
91. Bian, L., Hou, C., Tous, E., Rai, R., Mauck, R. L., & Burdick, J. A. The influence of hyaluronic acid hydrogel crosslinking density and macromolecular diffusivity on human MSC chondrogenesis and hypertrophy. *Biomaterials* (2013) 34: 413-421. doi: 10.106/j.biomaterials.2012.09.052
92. Leach, J. B. & Schmidt, C. E. Characterization of protein release from photocrosslinkable hyaluronic acid-polyethylene glycol hydrogel tissue engineering scaffolds. *Biomaterials* (2005) 26:125-135. doi: 10.1016/j.biomaterials.2004.02.018
93. Jiang Y., Chen, J., Deng, C., Suuronen, E. J., & Zhong, Z. Click hydrogels, microgels, and nanogels: Emerging platforms for drug delivery and tissue engineering. *Biomaterials* (2014) 35: 4969-4985. doi: 10.1016/j.biomaterials.2014.03.001
94. Li, G. Randev, R. K., Soeriyadi, A. H., Rees, G., Boyer, C., Tong, Z., Davis, T. P., Becer, R., and Haddleton, D. M. Investigation into thiol-(meth)acrylate Michael addition reactions using amine and phosphine catalysts. *Polymer Chemistry* (2010) 1: 1196-1204. doi: 10.1039/c0py00100g

95. Jin, R., Moreira Teixeira, L. S., Krouwels, A., Dijkstra, P. J., van Blitterswijk, C. A., Karperien, M., & Feijen, J. Synthesis and characterization of hyaluronic acid-poly(ethylene glycol) hydrogels via Michael addition: an injectable biomaterial for cartilage repair. *Acta Biomaterialia* (2010) 6: 1968-1977. doi: 10.1016/j.actbio.2009.12.024
96. Grim, J. C., Brown, T. E., Aguado, B. A., Chapnick, D. A., Viert, A. L., Liu, X., & Anseth, K. S. A reversible and repeatable thiol-ene bioconjugation for dynamic patterning of signaling proteins in hydrogels. *ACS Central Science* (2018) 4: 909-916. doi: 10.1021/acscentsci.8b00325
97. Lowe, A. B. Thiol-ene "click" reactions and recent applications in polymer and material synthesis. *Polymer Chemistry* (2010) 1:17-36. doi: 10.1039/b9py00216b
98. Nair, D. P., Podgorski, M., Chatani, S., Gong, T., Xi, W., Fenoli, C. R., & Bowman, C. N. The thiol-Michael addition click reaction: a powerful and widely used tool in material chemistry. *Chemistry of Materials* (2014) 26: 724-744. doi: 10.1021/cm402180t
99. Bencherif, S.A., Srinivasan, A., Horkay, F., Hollinger, J.O., Matyjaszewski, K., & Washburn, N.R. Influence of the degree of methacrylation on hyaluronic acid hydrogels properties.*Biomaterials*. 2008 Apr; 29(12):1739-49. doi:10.1016/j.biomaterials.2007.11.047
100. Wang, C., Tong, X., & Yang, F. Bioengineered 3D brain tumor model to elucidate the effects of matrix stiffness on glioblastoma cell behavior using PEG-based hydrogels. *Molecular Pharmaceutics* (2014) 11: 2115-2125. doi: 10.1021/mp5000828
101. DeForest, C. A., Sims, E. A., & Anseth, K. S. Peptide-functionalized click hydrogels with independently tunable mechanics and chemical functionality for 3D cell culture. *Chemistry of Materials* (2010) 22:4783-4790. doi: 10.1021/cm101391y
102. Zuidema, J. M., Rivet, C. J., Gilbert, R. J. & Morrison, F. A. A protocol for rheological characterization of hydrogels for tissue engineering strategies. *Journal of Biomedical Materials Research Part B* (2014) 102B(5):1063-1073. doi: 10.1002/jbm.b.33088
103. Vanderhooft, J. L., Alcoutlabi, M., Magda, J. J., & Prestwich, G. D. Rheological properties of cross-linked hyaluronan-gelatin hydrogels for tissue engineering. *Macromolecule Biosciences* (2009) 9(1): 20-28. doi: 10.1002/mabi.200800141
104. Jha, A. K., Hule, R. A., Jiao, T., Teller, S. S., Clifton, R. J., Duncan, R. L. Pochan, D. J., & Jia, X. Structural analysis and mechanical characterization of hyaluronic acid-based doubly cross-lined networks. *Macromolecules* (2009) 42: 537-546. doi: 10.1021/ma8019442
105. Vinckier, A. & Semenza, G. Measuring elasticity of biological materials by atomic force microscopy. *FEBS Letters* (1998) 430:12-16. doi: 10.1016/S0014-5793(98)00592-4
106. Stolz, M., Raiteri, R., Daniels, A. U., VanLandingham, M. R., Baschong, W., & Aebi, U. Dynamic elastic modulus of porcine articular cartilage determined at two different levels of tissue organization by indentation-type atomic force

microscopy. *Biophysical Journal* (2004) 86: 3269-3283. doi: 10.1016/S0006-3495(04)74375-1
107. Alcaraz, J., Buscemi, L., Grabulosa, M., Trepat, X., Fabry, B., Farre, R., & Navajas, D. Microrheology of human lung epithelial cells measured by atomic force microscopy. *Biophysical Journal* (2003) 84:2071-2079. doi: 10.1016/S0006-3495(03)75014-0
108. Gavara, N. A beginner's guide to atomic force microscopy probing for cell mechanics. *Microscopy Research and Technique* (2017) 80:75-84. doi: 10.1002/jemt.22776
109. Kirmizis, D. & Logothetidis, S. Atomic force microscopy probing in the measurements of cell mechanics. *International Journal of Nanomedicine* (2010) 5:137-145. doi: 10.2147/IJN.S5787
110. Tripathy, S. & Berger, E. J. Measuring viscoelasticity of soft samples using atomic force microscopy. *Journal of Biomechanical Engineering* (2009) 131(9):094507. doi: 10.1115/1.3194752
111. Mckee, C. T., Last, J. A., Russel, P. & Murphy, C. J. Indentation versus tensile measurements of Young's modulus for soft biological tissues. *Tissue Engineering: Part B* (2011) 17(3):155-164. doi: 10.1089/ten.teb.2010.0520
112. Dimitriadis, E. K., Horkay, F., Maresca, J., Kachar, B., & Chadwick, R. S. Determination of elastic moduli of thin layers of soft material using the atomic force microscope. *Biophysical Journal* (2002) 82(5):2798-2810. doi: 10.1016/S0006-3495(02)75620-8
113. Jee, A. & Lee, M. Comparative analysis on the nanoindentation of polymers using atomic force microscopy. *Polymer Testing* (2010) 29:95-99. doi: 10.1016/j.polymertesting.2009.09.009
114. Oliver, W. C. & Pharr, G. M. Measurements of hardness and elastic modulus by instrumentation indentation: advances in understanding and refinements to methodology. *Journal of Materials Research* (2004) 19(1): 3-20. doi: 10.1557/jmr.2004.19.1.3
115. Rico, F., Rosa-Cusachs, P., Gavara, N., Farre, R., Rotger, M., & Navajas, D. Probing mechanical properties of living cells by atomic force microscopy with blunted pyramidal cantilever tips. *Physical Review E* (2005) 72:021914. doi: 10.1103/PhysRevE.72.021914
116. Bhardwaj, V., Harit, G. & Kumar, S. Interpenetrating polymer network (IPN): novel approach in drug delivery. *International Journal of Drug Delivery & Research* (2012) 4(3):41-54.
117. Park, Y. D., Tirelli, N. & Hubbell, J. A. Photopolymerized hyaluronic acid-based hydrogels and interpenetrating networks. *Biomaterials* (2003) 24:893-900
118. Suri, S. & Schmidt, C. E. Photopatterned collagen-hyaluronic acid interpenetrating polymer network hydrogels. *Acta Biomaterialia* (2009) 5:2385-2397. doi: 10.1016/j.actbio.2009.05.004
119. Buxboim, A., Rajagopal, K., Brown, A. E. X., & Discher, D. E. How deeply cells feel: method for thin gels. *Journal of Physics and Condensed Materials*. 2010 May; 22(19):. doi:10.1088/0953-8984/22/19/194116.

120. Williams, C. G., Malik, A. N., Kim, T. K., Manson, P. N. & Elisseeff, J. H. Variable cytocompatibility of six cell lines with photoinitiators used for polymerizing hydrogels and cell encapsulation. *Biomaterials* (2005) 26:1211-1218. doi: 10.1016/j.biomaterials.2004.04.024
121. Leach, J. B., Bivens, K. A., Patrick, C. W. & Schmidt, C. E. Photocrosslinked hyaluronic acid hydrogels: natural, biodegradable tissue engineering scaffolds. *Biotechnology and Bioengineering* (2003) 82(5):578-589. doi: 10.1002/bit.10605